

2 P
MIX

LIFE TESTING OF METAL-CERAMIC CO₂ LASERS

T. S. Fahlen
D. J. Radecki
R. S. Reynolds
R. Targ

GTE SYLVANIA, INC.
Mountain View, California 94040

November 1971

Final Report for Period February - October 1971

Prepared for
GODDARD SPACE FLIGHT CENTER
Greenbelt, Maryland 20771

Reproduced by
NATIONAL TECHNICAL
INFORMATION SERVICE
U S Department of Commerce
Springfield VA 22151

1602
N72-13440 (NASA-CR-122313) LIFE TESTING OF
METAL-CERAMIC CO₂ LASERS Final Report,
Feb. - Oct. 1971 T.S. Fahlen, et al (GTE
Sylvania, Inc., Mountain View, Calif.)
Unclas Nov. 1971 92 p CSDL 20E G3/16
11440

1. Report No.	2. Government Accession No.	3. Recipient's Catalog No.	
4. Title and Subtitle CO ₂ LASER TUBE LIFE TESTING AND FAILURE ANALYSIS		5. Report Date November 1971	6. Performing Organization Code
7. Author(s) R. S. Reynolds, D. J. Radecki, T. S. Fahlen, R. Targ		8. Performing Organization Report No. 465F	
9. Performing Organization Name and Address GTE Sylvania, Inc. Electro-Optics Organization P.O. Box 188 Mountain View, California 94040		10. Work Unit No.	11. Contract or Grant No. NAS5-21606
		13. Type of Report and Period Covered FINAL REPORT Feb. 1971 to Oct. 1971	
12. Sponsoring Agency Name and Address Goddard Space Flight Center Greenbelt, Maryland 20771 Technical Officer: John McElroy, 524		14. Sponsoring Agency Code	
		15. Supplementary Notes	
16. Abstract <p>The main purpose of this program was to determine the life characteristics of nine space-qualified, metal-ceramic CO₂ lasers. Lifetimes ranged between about 400 hours to over 2000 hours (the limit of testing) with a high degree of consistency in like groups. In all cases the tubes which had failed could be restored to near their original power by doubling the cathode current for 30 minutes. Periodic rejuvenation allowed operation for the full 2000 hours on all tubes. The failure mechanism appears to involve formation of NiO and C on the nickel cathode emission surface with subsequent adsorption of tube gases.</p>			
17. Key Words (Selected by Author(s)) CO ₂ LASER LIFE CO ₂ LASER FAILURE MECHANISMS SPACE QUALIFIED LASERS		18. Distribution Statement	
19. Security Classif. (of this report) UNCLASSIFIED	20. Security Classif. (of this page) U	21. No. of Pages 92	22. Price*

PREFACE

OBJECTIVE

The objective of this program was to determine the life characteristics of several metal-ceramic CO₂ lasers of a space qualified design built under strict fabrication and process controls.

SCOPE OF WORK

Nine metal-ceramic tubes of similar designs were constructed. These tubes were life tested under controlled conditions for a period of 2000 hours or until failure, whichever ever occurred first. One tube was shelf-life tested for 3000 hours. In addition nine all-glass tubes were constructed for a NASA-conducted life test program. Failure analysis was carried out for those tubes which had failed during the test program.

CONCLUSIONS

The basic tube design is capable of operation for 400-600 hours after which rejuvenation is required to maintain power output for periods of 2000 hours or more. Glass inserts in the metal-ceramic tube do not have an appreciable effect on life. Increasing the gas storage volume associated with the tube by a factor of 3 to 500 cc extends the tube life to well beyond 2000 hours without rejuvenation. Formation of NiO and carbon on the nickel cathode of the tube with subsequent adsorption of tube gases appears to be the major failure mechanism. No life limitations with storage were observed.

SUMMARY OF RECOMMENDATIONS

1. Preprocessing techniques for a nickel cathode should be developed.
2. For tube lifetimes of 10,000 hours or more, a new cathode material should be developed.
3. Studies should be continued on the development of a controllable CO₂ gas generator to automatically replace the CO₂ lost in chemisorption as the tube is operated.

TABLE OF CONTENTS

<u>Section</u>	<u>Title</u>	<u>Page</u>
1	INTRODUCTION	1
2	METAL-CERAMIC CO ₂ LASER EFFORTS	3
2.1	TUBE DESIGN SUMMARY	3
2.2	DESCRIPTION OF LIFE TEST TUBES	8
2.2.1	<u>Introduction</u>	8
2.2.2	<u>Precursor Tube</u>	9
2.2.3	<u>Standard Tubes</u>	10
2.2.4	<u>Glass Insert Tubes</u>	11
2.2.5	<u>Ballast Tubes</u>	13
2.2.6	<u>Tube Overfilled with CO₂</u>	15
2.3	LIFE TEST PROGRAM	15
2.3.1	<u>Introduction</u>	15
2.3.2	<u>Life Test Station</u>	16
2.3.3	<u>Life Test Procedures</u>	19
2.3.4	<u>Life Test Results</u>	
2.4	FAILURE ANALYSIS	32
2.4.1	<u>Introduction</u>	32
2.4.2	<u>Residual Gas Analysis</u>	33
2.4.3	<u>Optical Tests</u>	39
2.4.4	<u>Chemical, Spectroscopic, and Related Tests</u>	40
2.4.5	<u>Proposed Failure Mechanism</u>	46
2.4.6	<u>Metal-Ceramic Brazing Failures</u>	49
2.5	RELATED RESEARCH	51
2.5.1	<u>Introduction</u>	51
2.5.2	<u>Zeolite as a Water Source</u>	52
2.5.3	<u>Nickel Carbonate as a CO₂ Source</u>	63
2.5.4	<u>Vibration Tests on Glass-Center-Section Tube</u>	64
3	ALL-GLASS CO ₂ LASER TUBES	69
3.1	INTRODUCTION	69
3.2	<u>GLASS TUBE DESIGN</u>	69

TABLE OF CONTENTS

<u>Section</u>	<u>Title</u>	<u>Page</u>
3.3	GLASS LIFE TEST LASERS	73
4	LASER CONTROL ELECTRONICS	77
4.1	INTRODUCTION	77
4.2	SUMMARY OF ELECTRONICS SPECIFICATIONS	77
4.3	STABILIZATION ELECTRONICS TEST RESULTS	79
5	CONCLUSIONS AND RECOMMENDATIONS	85
6	NEW TECHNOLOGY	89
7	REFERENCES	91
	APPENDIX	92

LIST OF ILLUSTRATIONS

<u>Figure</u>	<u>Caption</u>	<u>Page</u>
1	Ceramic laser tube assembly	4
2	Standard metal-ceramic CO ₂ laser tube	5
3	View of metal-ceramic CO ₂ laser subassemblies	7
4	Glass insert tube detail	12
5	Photo of ballast tubes	14
6	Life test station	17
7	Life test results on standard tube (MIL-STD-5)	22
8	Life test results on standard tube (MC-STD-6)	23
9	Shelf life test results for standard tube (MC-STD-7)	24
10	Life test results for tube with 50% overfill of CO ₂ (MC-STD-8)	25
11	Life test results for tube with glass insert (MC-GI-1)	26
12	Life test results for tube with glass insert (MC-GI-2)	27
13	Life test results for tube with glass insert (MC-GI-3)	28
14	Life test results on tube with ballast tank (MC-B-1)	29
15	Life test results on tube with ballast tank (MC-B-2)	30
16	Life test results on precursor tube (R*D 1)	31
17	Gas analysis system	35
18	Photograph of sampling valve	36
19	Photograph of a nickel cathode after 2,000 hours of operation	41
20	Cathode RGA tester	43
21	RGA results of desorption measurements on used cathode	45
22	Metal-ceramic tube-end subassembly	50
23	Water vapor absorbed by Linde Type 4A molecular sieve vs. vapor pressure (from Linde data sheet No. 4A-1, 11-27-57)	55

LIFE OF ILLUSTRATIONS

<u>Figure</u>	<u>Caption</u>	<u>Page</u>
24	Zeolite heater assembly	59
25	Zeolite oven controller	60
26	Zeolite tube parameters vs. discharge time	62
27	Pressure increase resulting from heating NiCO_3	65
28	Glass center section tube used for window testing	66
29	Glass life test tube	70
30	Photograph of all-glass tube	71
31	Assembly drawing of aluminum heat sink	72
32	Completed glass life test laser with optical cavity	74
33	Frequency stabilization electronics	78
34	Photograph of the laser control electronics, front view	80
35	Photograph of the laser control electronics, rear view	81

LIST OF TABLES

<u>Table No.</u>	<u>Title</u>	<u>Page</u>
1	Metal-ceramic life test tubes designation and description	9
2	Life of operating hours to failure for metal-ceramic life test tubes	20
3	RGA results for life test tubes	37
4	Glass life test tubes and their life test variables	75
5	Major interface specifications	79
6	Power supply currents	82

SECTION I

INTRODUCTION

In November, 1969 the NASA-Goddard Space Flight Center initiated a program for the development, fabrication and test of a CO₂ laser communications experiment (LCE) to be flown on the ATS-F satellite. The Aerojet General Corporation was chosen as the prime contractor for this effort. One of the objectives of that program was the measurement, through formal and controlled testing, of the lifetime characteristics of the space qualified tubes developed for the LCE. Early termination of the program, however, precluded such testing.

As a natural outgrowth of the LCE program the effort to be reported here was started in February 1971 and was specifically directed toward obtaining knowledge of the life characteristics and hopefully the failure mechanisms for the tube designs which were being considered for the LCE. This program is therefore primarily concerned with the fabrication and life-test of several CO₂ laser tubes of an earlier design already proven capable of withstanding the environmental requirements of the ATS-F satellite.

As part of the LCE efforts, detailed fabrication and process controls were developed for the tubes along with specialized jigs used in fabrication and sub-component testing. These were developed in order to ensure uniformity in all phases of fabrication, to increase yield and, hopefully to provide uniform operating characteristics from tube to tube. Since these formal controls were utilized with the tubes fabricated on this current program, the degree of consistency in life test results from tubes with the same design parameters will also provide information as to the adequacy of the controls.

Although the main purpose of this program was the fabrication and life test of several tubes designed for the LCE, other related activities were pursued and are reported herein. In addition to the LCE type of tube, several all-glass tubes of a NASA design were fabricated. Earlier efforts⁽¹⁾ have indicated that small amounts of water vapor in the laser mix may be

beneficial to tube life and that the glass used in the tube construction may be able to provide the quantity of water vapor required. A total of nine all-glass tubes of a space qualified design were fabricated, processed and delivered to NASA for life testing.

In addition, since the metal-ceramic type tube may not have the same water vapor absorption characteristics as glass, and most likely has a very low affinity towards water vapor, a limited amount of research was performed on the water vapor storage capability of various types of Zeolite, an additive which could be placed inside the metal-ceramic CO₂ laser tube envelope. Studies were performed on the adsorption and desorption characteristics of Zeolite as a function of temperature, partial pressures of gases and of the quantity of Zeolite required with respect to the total tube volume. Nickel carbonate was also studied briefly as a possible solid state source of CO₂.

A task unrelated to tube life was also performed on the program and is reported in a later section. It involved the completion of fabrication and testing of an electronic control box designed under the earlier LCE program to automatically control the laser frequency by a "dither" control technique. This automatic frequency control unit is planned for use on NASA in-house CO₂ laser efforts.

The remainder of this report is organized into three major technical subsections covering the metal-ceramic tube efforts, the glass tube efforts and the AFC electronics efforts in Section 2, 3, and 4 respectively. Conclusions and recommendations are covered in Section 5 with new technology and references contained in Sections 6 and 7.

SECTION 2

METAL-CERAMIC CO₂ LASER EFFORTS

This section will cover the efforts applied to the metal-ceramic tubes. The design of the standard tube will be briefly reviewed after which more detailed discussions on the life test procedures, results and analysis will be covered.

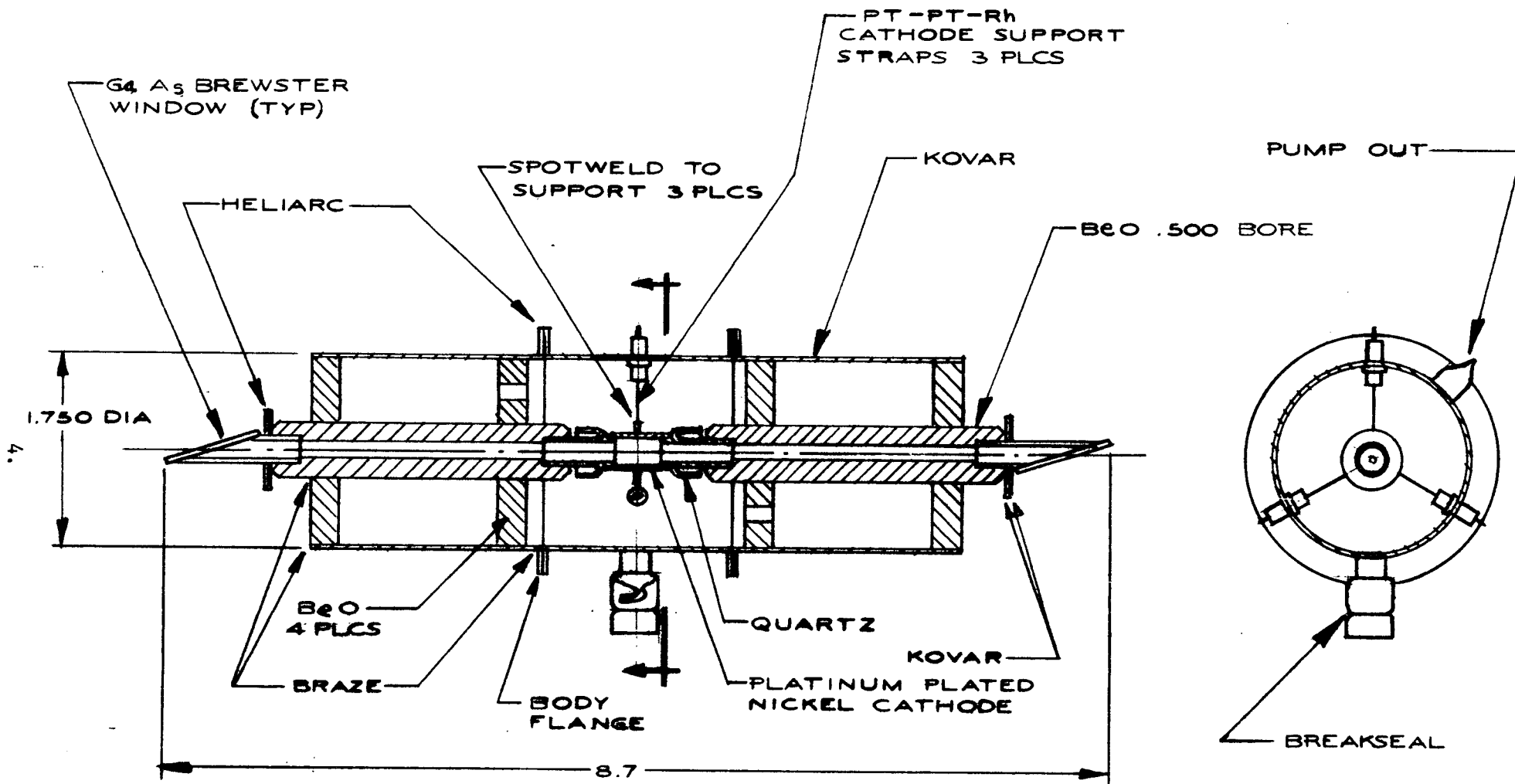
2.1 TUBE DESIGN SUMMARY

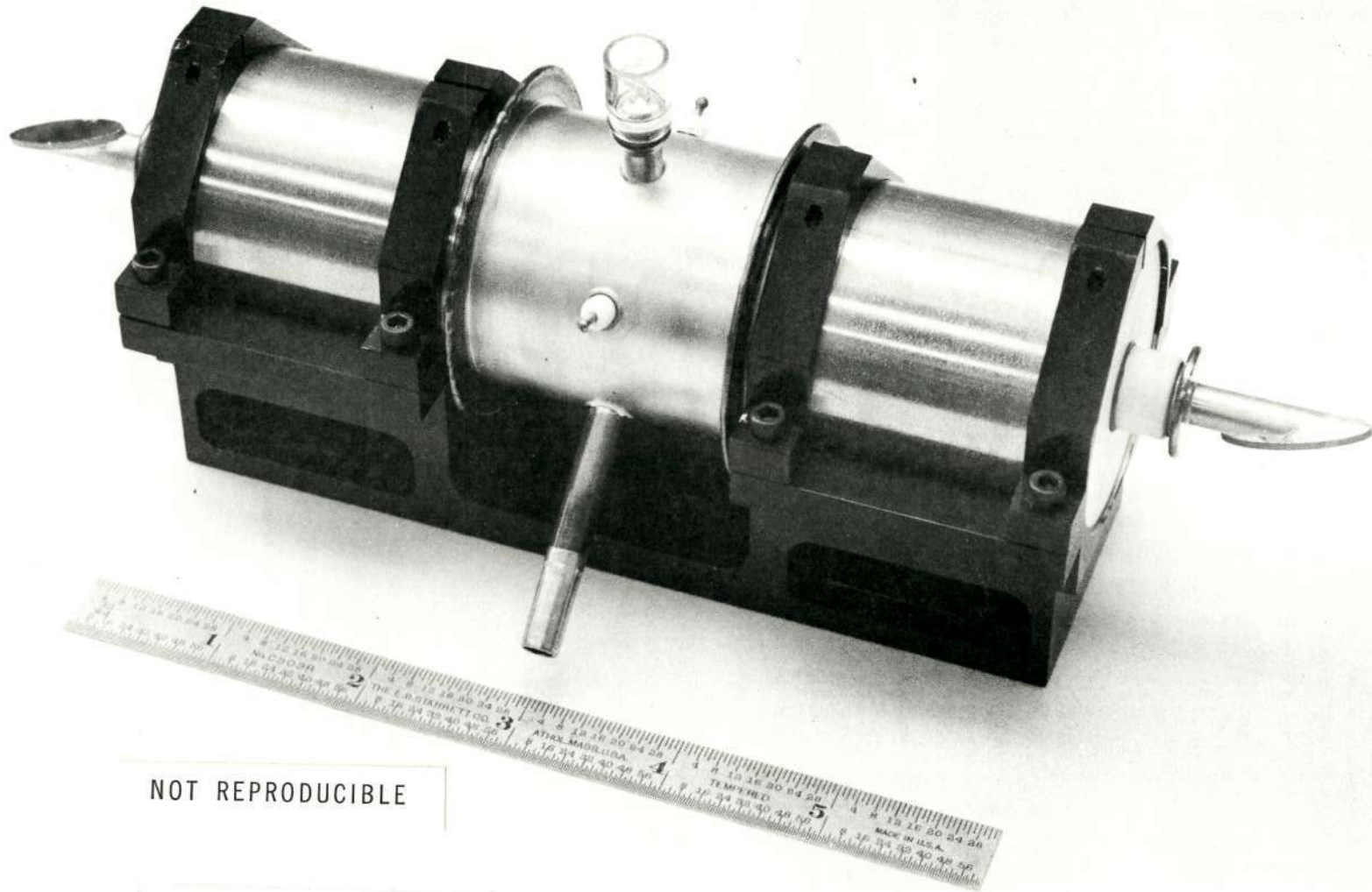
Figure 1 shows a cross-sectional view of the basic metal-ceramic laser tube built on the current program. Figure 2 is a photograph of a completed tube in its mating heat-sink. This tube was first designed by GTE Sylvania for the NASA - Electronics Research Center on Contract NAS12-2021 entitled Space Qualified CO₂ Laser. The tube was developed further under a contract with the Aerojet-General Corporation for the NASA-Goddard Space Flight Center Laser Communications Experiment.

The laser tube design is based on the following set of major parameters:

- a. The tube must be of sufficient length to provide enough gain for 1W minimum output power at the maximum environmental temperature.
- b. The tube must operate with conduction cooling.
- c. The tube must operate with a heated cathode (for long life).
- d. The tube must provide TEM₀₀ power only.
- e. The output beam must be polarized.
- f. The tube must have a long operating life.
- g. The tube must be bakeable.
- h. The tube must be rugged to withstand environmental conditions.
- i. The tube should have as high an operating efficiency as possible.

Figure 1 Ceramic laser tube assembly





NOT REPRODUCIBLE

Figure 2 Standard metal-ceramic CO₂ laser tube

A few of the more salient features of the design are listed below.

- a. The tube has circular geometry with a 4.25 mm diameter bore made of beryllium oxide. Four 1/4 inch thick BeO fins are located along the tube bore. BeO is used because of its very high coefficient of thermal conductivity, making the heat transfer characteristics of the tube exceptional.
- b. The outside shell, made of thin-walled nickel-plated Kovar, serves as a rigidizing structure as well as the vacuum envelope. The spaces between the BeO fins provide a ballast volume of approximately 150 cc.
- c. The tubes are of modular design so that flexibility and variety in construction is possible in order to obtain slightly different operating parameters. Each tube consists of six main subassemblies; two Brewster window assemblies, two tube-end assemblies, a cathode assembly, and a center section. The fabrication of each subassembly is strictly controlled by a process specification. Figure 3 is a photograph of the subassemblies.
- d. For maximum tube efficiency, the laser utilizes a coaxial electrode structure rather than electrodes in side arms. The kovar pieces at each end of the laser tube serve as anodes while the nickel cylinder (platinum plated on outside surface) in the center of the tube is the tube cathode. The cathode is heated to at least 250°C during operation. To achieve this without requiring additional external heat, the cathode has been isolated from the BeO bore by insulating sections of quartz glass. To provide the electrical connection to the cathode, as well as additional support, three thin wires of platinum run between the cathode and the outside surfaces of the tube. One of the platinum wires contains rhodium which forms a thermocouple junction at the cathode allowing the cathode temperature to be monitored. The wires are terminated on an insulating ceramic feed-through so that the cathode may be operated somewhat above ground potential if required. The advantages of a two anode,

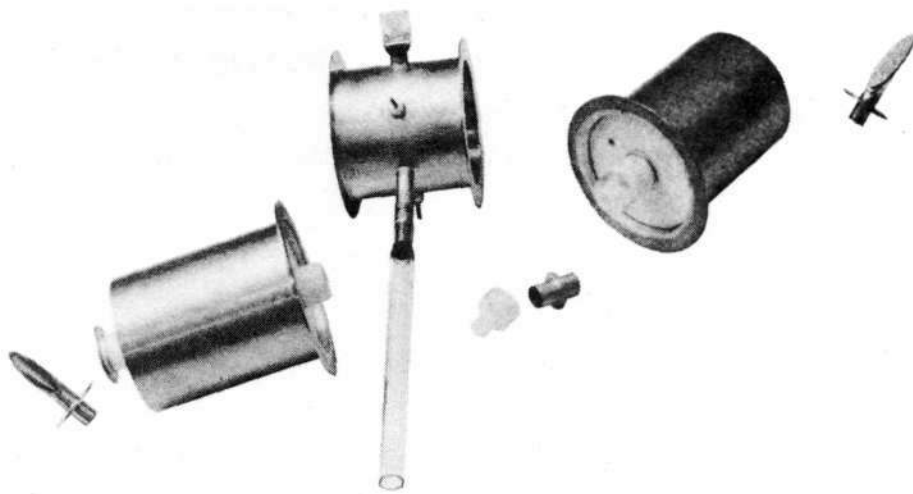


Figure 3 View of metal-ceramic CO₂ laser subassemblies

single cathode approach over a single cathode, single anode approach are:

1. Sputtered material from the cathode is kept farther from the laser windows
 2. Total tube voltage is approximately halved
 3. Greater power is dissipated at the cathode, since twice the current is being drawn, enabling the cathode to be self-heating.
- e. The gallium arsenide Brewster windows are attached to the end Kovar assemblies using hard soldering techniques, allowing rugged ultra-high-vacuum seals to be obtained. The window assemblies (which are prepared independent of the tube) are then oriented and heliarc-welded to the tube at the appropriate point in the tube fabrication cycle. Each window assembly is tested prior to installation on the tube in a laser test fixture capable of detecting window losses as low as 0.1 percent.

2.2 DESCRIPTION OF LIFE TEST TUBES

2.2.1 Introduction

Prior to the fabrication of nine metal-ceramic life test tubes, a precursor tube was assembled using tube ends and a center section which had been used previously. The purpose of this tube was to aid in finalizing the process specifications which had not yet been completed. The tube was also life tested to gain some assurance that the process controls were adequate. Subsequently, the nine life test tubes were built, incorporating five design variables into the fabrication and processing of the tubes.

Other than these variations, the tubes were made identically, according to the same process specifications. Three tube types were constructed in order to investigate the five variables, a standard tube, a standard tube with a glass insert, and a standard tube with an extra gas ballast. Table 1 lists the nine tubes built, their designation, and the design variable. Each tube was fixed in an aluminum mount which was

TABLE I

Metal-Ceramic Life Test Tubes Designation and Description

<u>No.</u>	<u>Designation</u>	<u>Description</u>
1	MC-STD-5	Standard tube
2	MC-STD-6	Same as 1
3	MC-STD-7	Same as 1 except shelf-life test only
4	MC-STD-8	Contained 50% extra CO ₂
5	MC-GI-1	Contained 90 cm ² pyrex glass insert
6	MC-GI-2	Same as 5
7	MC-GI-3	Same as 5
8	MC-B-1	Contained 350 cc additional ballast. Cathode current = 12 ma
9	MC-B-2	Same as 8 except cathode current = 9 ma

assigned to the tube parts during fabrication. The aluminum mount serves as an assembly jig during fabrication, and as a sink for removal of heat from the tubes during operation. In addition, each tube has a small glass break-seal which provides a means of sampling the gas after failure.

The following sections will deal with some of the details of the different life test variables.

2.2.2 Precursor Tube

As stated previously, the precursor tube served as a check of several newly developed processes and techniques which were originated on other programs. It was a standard tube of the type described generally in Section 2.1.

All of the fabrication controls were firmly developed prior to assembly of the precursor tube, except for the final gas processing procedure. This tube served as the vehicle for the completion of the processing specification.

The tube was then life-tested to determine if there were any major problems affecting tube-life which could be corrected before the beginning of the life tests on the nine formal life test tubes.

2.2.3 Standard Tubes

MC-STD-5, 6, and 7 were standard tubes of the type shown earlier in Figure 2. They were fabricated exactly according to the process specifications, except for two instances where equipment malfunctions resulted in poor heliarc welds. These welds had to be removed and redone. To protect against the case where variances on the fabrication procedures might lead to a compromise in the goals of the program, an internal material review board was convened whenever fabrication or processing required deviation from the process specifications. A fabrication log was kept for each tube where tube fabrication details were recorded.

MC-STD-7 was shelf life tested to determine if gas permeation through the tube envelope, contamination, or chemical effects were of significant magnitude to be detrimental to tube life through extended storage periods. After an initial break-in period of 170 hours it was operated for only four hours per week for the duration of its test. MC-STD-5 and MC-STD-6 were operated continuously for the duration of their test (2000 hours).

Extensive parametric studies had been done on an earlier program on five-component gas mixtures for the metal ceramic tube. During these studies power output was optimized as a function of gas pressure and mixture. It was found that a gas mixture containing 0.2 Torr H₂, 0.1 Torr O₂,

7.0 Torr N₂, 8.0 Torr CO₂, and 15.0 Torr He provided a good compromise between maximum power and maximum efficiency and this mixture became the standard mix for this program.

2.2.4 Glass Insert Tubes

Since the first metal-ceramic tubes were built, there have been many questions raised as to whether their materials were compatible with long life. Glass tubes had been built by Sylvania as well as others which had demonstrated thousands and even tens of thousands of hours of operational life-time, yet few, small volume, metal-ceramic tubes had operated for more than a few hundred hours. Those which had lasted for longer periods had either large ballast volume, substantial glass surface area exposed to the gases, or both. Theories had developed connecting the use of glass in tubes with long life primarily based on the fact that glasses have a high affinity for water vapor and could provide a source of water vapor for the laser tube. Small amounts of water-vapor or hydrogen were believed to be beneficial to tube life because they produce a higher equilibrium CO₂ pressure in the tube by reducing the dissociation rate of CO₂ in the discharge.⁽¹⁾

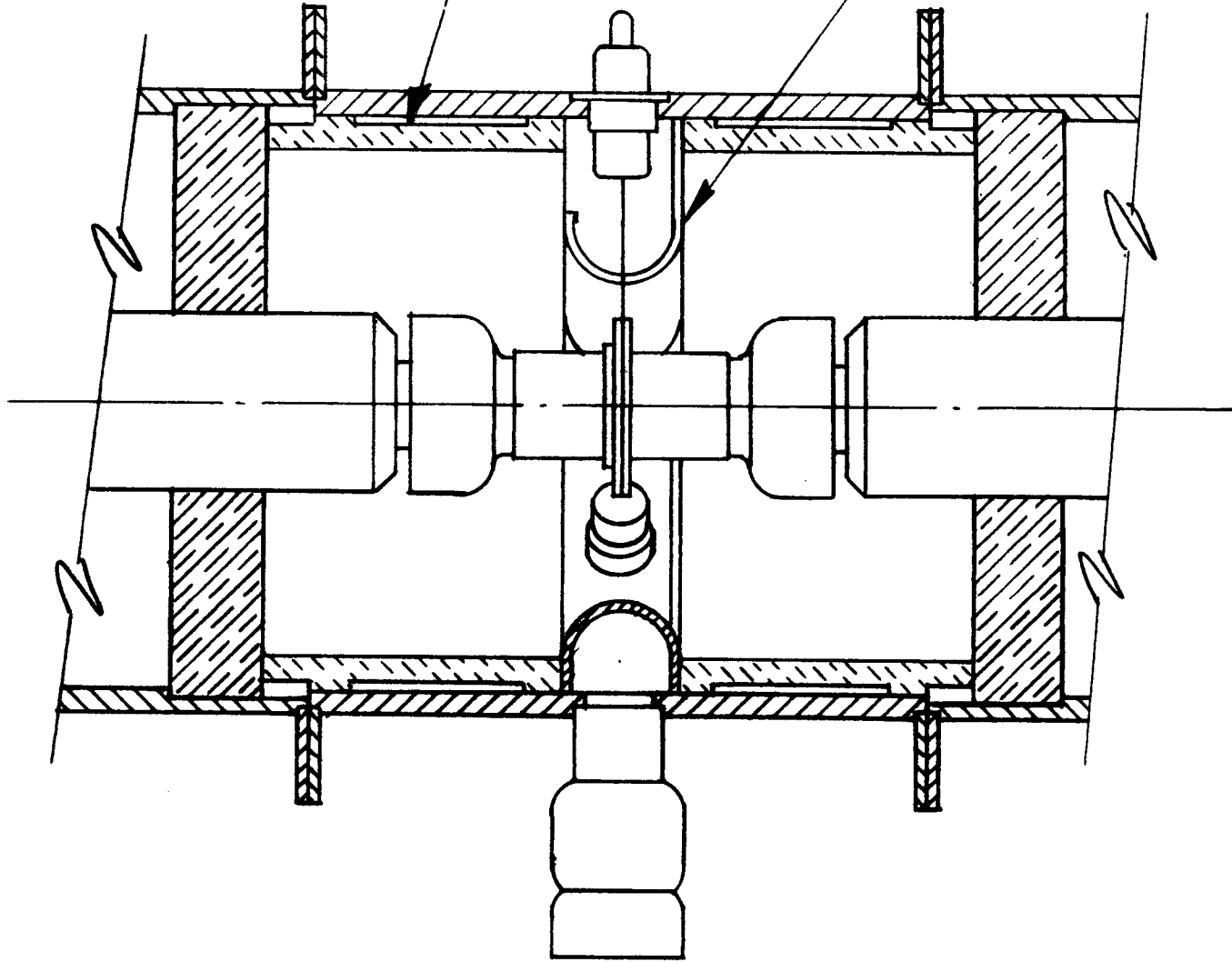
The glass insert tubes were designed to provide the answer to the question of whether glass was necessary for long life or not.

The glass inserts were designed so they could be installed in a standard tube without any modifications, prior to final assembly. Figure 4 shows a cross-sectional view of the glass inserts installed in the center section of a standard tube. The design consists of two separate pyrex glass cylinders which are slipped inside the standard center section from each end. A Kovar spring made from .015 inch sheet is placed between the cylinders to force them against the tube end assemblies (BeO fins). The outside diameters of the glass cylinders are accurately ground to mate with the inside diameter of the Kovar center section. Although this design was itself not vibrated we believe that, based on tests conducted on a similar glass insert, this design is satisfactory for space environment use. The glass surface area exposed to the gas mixture is approximately 90 cm².

Figure 4 Glass insert tube detail

PYREX GLASS INSERT

KOVAR SPRING



MC-GI-1 and MC-GI-2 were fabricated and processed according to the process specifications. MC-GI-3 was also fabricated and processed according to the specifications except that in order to maintain schedule, two tube ends with very small leaks had to be used. The leaks were sealed with a high vacuum sealant and the assembly and processing proceeded normally. The leaks occurred in a particular ceramic-to-ceramic braze joint and became a recurring problem on some later tubes. The problem and its solution will be discussed in Section 2.4.7.

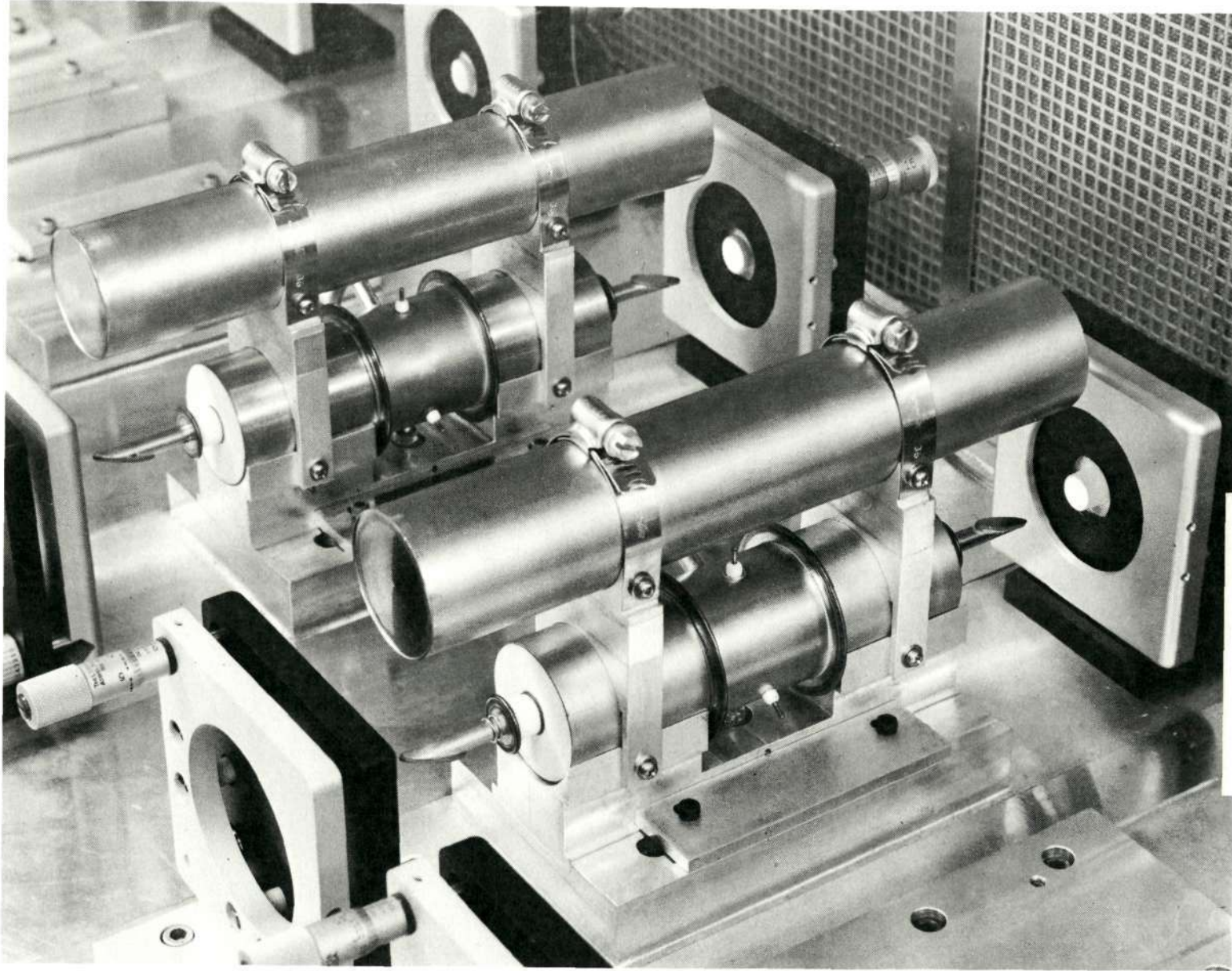
All three glass-insert tubes were operated continuously throughout the duration of their testing.

2.2.5 Ballast Tubes

It had been known for some time that if gas cleanup was prevalent in a CO₂ laser tube, then the life of the tube could be extended by increasing its gas storage volume. The rate at which CO₂ disappears from the tube varies depending on tube materials, tube geometry, cathode design, and many other factors, making the cleanup rate a very complex function of tube design. The purpose of the ballast tubes then was to gain insight to the question of how tube life varies with storage volume. As will be discussed later, it is not necessarily linear.

Figure 5 shows a photograph of the two ballast tubes, MC-B-1 and MC-B-2 constructed for life test. The ballast tank is mounted directly over the top of the tube. It is made of 1.67 inch I.D. Kovar and is approximately 9.5 inches in length, providing an additional ballast including tubulations of 350 cc making the total tube volume about 500 cc. The tanks are attached to the tubes using aluminum brackets. The final braze of tube to ballast tank makes the entire structure very rigid. Although no vibration tests were run on this design, we believe that this design could be qualified for space use.

The fabrication and processing of MC-B-1 and MC-B-2 went well except for the continued brazing problem. Because of the vendor's inability to supply leak tight tube-end assemblies, tube ends originally



NOT REPRODUCIBLE

Figure 5 Photo of ballast tubes

brazed for the ATS-LCE were used for MC-B-2. They were leak tight, but were approximately 0.1 inch shorter than the standard life test tubes. All other aspects of this tube were the same as the standard tubes. Both tubes were run continuously during their test. In order to study the affect of tube current on tube life, MC-B-1 was run at 12 ma total current and MC-B-2 at 9 ma.

2.2.6 Tube Overfilled with CO₂

Based on experience obtained with a metal-ceramic development tube fabricated on a previous program and early results obtained on NASA's glass tubes, it was decided that the final tube built on the program should be filled with additional CO₂. The earlier development tubes which had used extra CO₂ had all lived longer than similar tubes with standard mixes.

The standard tube, MC-STD-8, was fabricated and processed according to the specifications but was filled with 12 Torr of CO₂ rather than 8 Torr as in the standard mix. (See Section 2.2.3.) With 50% additional CO₂ available, the lifetime was expected to be increased for reasons similar to those favoring additional ballast volume. Because of the increased total pressure, however, the power output history would not be necessarily similar to that of a tube with 50% extra volume.

Tests were conducted which showed that 50% more CO₂ could be added without decreasing the power output by more than 20% from the maximum obtainable using a standard mix.

This tube was operated at 10 ma total current for 110 hours at which time the current was decreased to 9 ma. It was then run continuously at that level for the duration of its life test.

2.3 LIFE TEST PROGRAM

2.3.1 Introduction

The purpose of this program was to life test nine metal-ceramic tubes with controlled design variables, as described in the previous section, in order to establish their fundamental lifetimes.

In order to be accepted for life test, each tube was required to demonstrate a minimum power output of 800 mW. The power output measurements were made during processing in a standard processing cavity with an 11% transmitting output mirror and a 60 cm radius of curvature non-output mirror. Each tube demonstrated 1.35 watts \pm 0.1 watts in this cavity, indicating the consistency in their fabrication. As will be discussed in the following section, a 4% \pm 1% transmitting output mirror was used in the life test cavities which reduced their power output to near 800 mW. Mirror transmission, mixture, and operating current variations accounted for minor power output variations at the start of the life test.

The power output, current, operating voltage, and cathode temperature for each tube were monitored during the life test. As mentioned previously, different tubes had different operating currents. The standard operating current was changed during the course of the program from 9 ma to 12 ma for reasons which will be discussed in later sections. In addition, the heat sink temperature was held constant at $19^{\circ}\text{C} \pm 1^{\circ}\text{C}$ and verified by periodic monitoring.

The life-test duration for each tube, with the exception of MC-STD-8, MC-B-1 and MC-B-2 was three months (\sim 2160 hours), unless prior failure occurred. Failure was defined as when the tube's power output fell to 25% of its initial power output in the life test cavity.

Upon failure, the final gas mixture for each tube was to be analyzed and further analysis conducted as appropriate to determine the failure mechanism.

The following sections will describe the life-test facility, procedures, and failure analyses, and present some of the conclusions drawn from the analysis.

2.3.2 Life Test Station

Figure 6 is a photograph of the life test station. The station consists of a power-supply rack, and a water-cooled aluminum baseplate for the laser tubes mounted in a laminar flow bench. The aluminum base plate

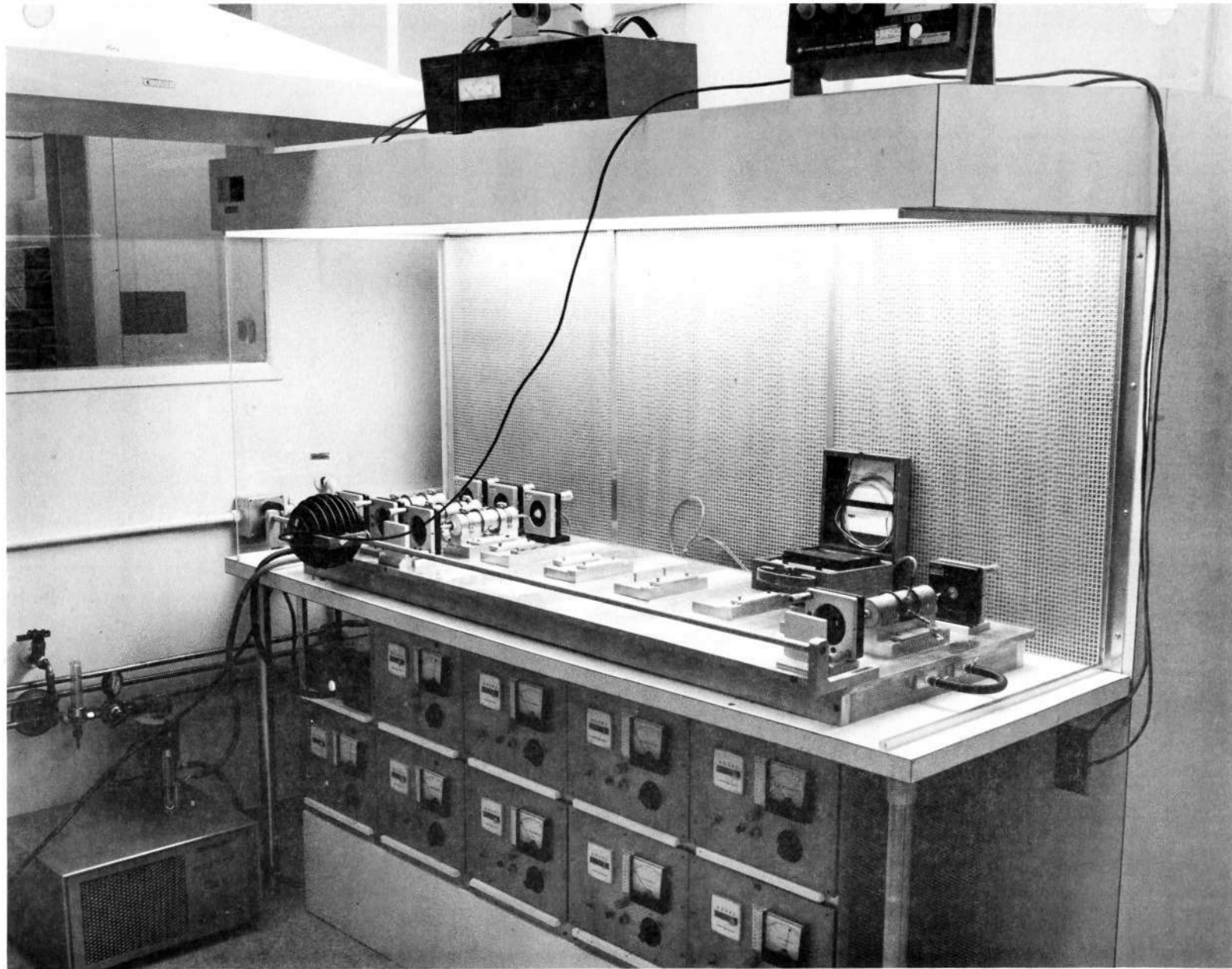


Figure 6 Life test station

has nine milled flats with locating blocks which align each tube precisely in the center of each cavity. The optical cavity is formed by a flat 4% + 1% transmitting output mirror, and a 60 cm radius of curvature metal-dielectric coated non-output mirror mounted on a piezoelectric transducer. A 4% output transmission was chosen so that the lasers would be somewhat undercoupled. The baseplate has water cooling lines welded to its underside. A traverse rod is provided on which a Coherent Radiation power meter head can slide and be positioned in front of each laser for power measurements. The locating blocks and fasteners are designed to hold the standard tube mount rigidly. Silicone heat sinking compound is used to insure good thermal contact between the tube mount and the milled flat on the baseplate.

The power supply for each tube provides 15,000 VDC at 15 ma maximum. The main power to the supplies was wired through a water-pressure switch so that in the event of a water cooling failure the tubes would be turned off.

A Lansing lock-in stabilizer was used as an aid in making consistent power output measurements and in aligning the laser cavity for peak output power.

The life test station was placed on a laminar flow bench to ensure a dust free operating environment for the tubes, relieving any requirements for cleaning the cavity optics for the duration of the life test. Earlier experience had shown that the cleaning of these optics frequently could degrade them and cause increased cavity losses resulting in a power loss not attributable to fundamental failure mechanisms. In addition dust could be burned into the optical surfaces causing permanent damage.

The laminar flow bench provided a measured dust count level of less than 100 particles/ft³ of greater than 1/2 μ size. This is much lower than the earlier established number of 10,000 particles/ft³ required to eliminate the need for periodic cleaning during the time period of this test.

2.3.3 Life Test Procedures

In order to obtain uniformity in data taking, a standardized procedure was established. The tube power, voltage, and cathode temperature were measured daily for the first two weeks. As an operating trend was established for each tube, measurements were taken less frequently depending on the rate of change of tube power. Baseplate temperature was also monitored.

The standard procedure for taking data is listed below:

- 1) Block the beam and zero the power meter.
- 2) Check the tube operating current and reset if necessary.
- 3) Dither the non-output mirror using the fast sweep of transducer control.
- 4) Remove block and while dithering adjust front mirror for maximum power.
- 5) Turn off sweep and manually scan mirror through its entire range (15 microns).
- 6) Record maximum power observed.
- 7) Measure tube voltages between both anodes and ground.
- 8) Measure and record baseplate temperature.
- 9) Measure and record cathode thermocouple voltage and convert to temperature.
- 10) Record elapsed hours shown on meter.

The same calibrated test equipment was used throughout the program.

Several tubes fell below their 25% power level prior to the end of the 2000 hour test period. As part of the failure analysis a tube "rejuvenation" process was performed on these tubes. The rejuvenation procedure consisted of increasing the tube current to approximately 15 ma until the cathode temperature was over 400°C. The tube current was left at this high value until 1) the power output began to rise, and 2) the cathode temperature reached a maximum, began to fall slowly, and leveled off at some lower temperature. The rejuvenation process usually took between 10 and 20 minutes and in every case the tube's initial power output

could be restored. Tube voltage, and cathode temperature were recorded during the rejuvenation cycles.

The compiled data was kept in a running log and plotted in graphical form.

2.3.4 Life Test Results

Figures 7 through 16 show the data compiled on the precursor and nine life-test tubes. For the most part, they are self explanatory; however, a few points will be briefly discussed.

Table 2 is a summary of the life times determined for the nine tubes on the program. The lifetimes given are those technically defined for the program. However, it should be noted that useful power output was obtained from all the tubes for 2000 hours by the rejuvenation process used.

TABLE 2

LIST OF OPERATING HOURS TO FAILURE FOR METAL-CERAMIC LIFE TEST TUBES

Tube	Time to 25% power level (hours)
MC-STD-5	460
MC-STD-6	720
MC-STD-7	> 3000 (shelf-life)
MC-STD-8 (50% CO ₂ overfill)	805
MC-GI-1	410
MC-GI-2	460
MC-GI-3	475
MC-B-1	> 2000
MC-B-2	> 2000

The spikes in the cathode temperature curve represent a rejuvenation cycle. Some tubes required rejuvenating less frequently than others. With each rejuvenation there is a corresponding increase in power output. MC-STD-5, MC-GI-2, and MC-GI-3 required rejuvenating far more often than MC-STD-6 and MC-GI-1. The ballast tubes MC-B-1 and MC-B-2 never required

rejuvenation. After the first few attempts at rejuvenating MC-STD-5 and MC-STD-6 it was decided to increase the cathode temperature by increasing the tube current on all tubes that had technically failed, to determine if the elevated cathode temperature would lengthen the time span between rejuvenation cycles. Examination of the graphs indicates it was helpful in some instances and not in others.

MC-STD-7, the shelf-life tube, showed only minor power variations during its 3000 hour test. There is a definite correlation between power output and cathode temperature for this tube. However, this is probably due to small variations in operating current. The tube was operated for 170 hours initially and then once a week for 4 hours thereafter. It had a final total of 3000 shelf-life hours and 255 operating hours.

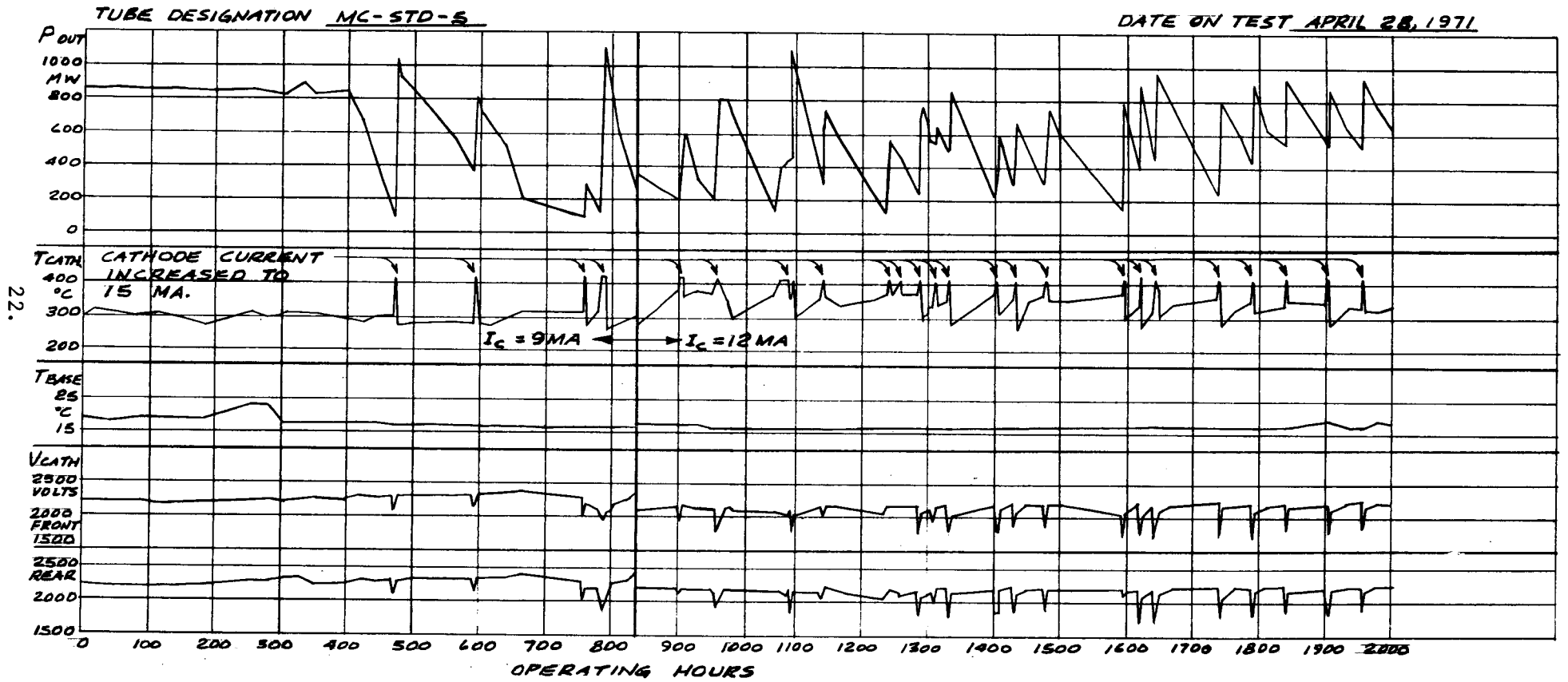
Four out of five of the other standard and glass insert tubes fell below their 25% power point between 400 and 500 hours. For some reason not attributable to any known fabrication or processing differences, MC-STD-6 went for 720 hours. Except for this one variance, all of the like tubes failed in a time very close to each other providing credibility to the fabrication and process controls.

The ballast tubes did not fail within the 2000 hours of required testing. Therefore, no rejuvenation efforts were attempted. Both tubes however, decreased in output power to approximately 75% of their original power. The life curves indicate no substantial difference in life between the case of 9 ma and 12 ma tube current.

The CO₂ over-fill tube, which had approximately 1.5 times more CO₂ molecules initially than did the standard tubes, failed at approximately 800 hours. We continued rejuvenation and recording data only until 1000 hours since the rejuvenation data was similar to that seen on earlier tubes.

Having glass present in the glass insert tubes did not increase their lifetime or alter their operating characteristics appreciably. The glass, however, apparently did maintain a higher H₂ and CO₂ content in the tubes as compared to a standard tube as will be seen in the next section.

Figure 7 Life test results on standard tube (MIL-STD-5)



TUBE DESIGNATION MC-STD-6

DATE ON TEST APRIL 28, 1971

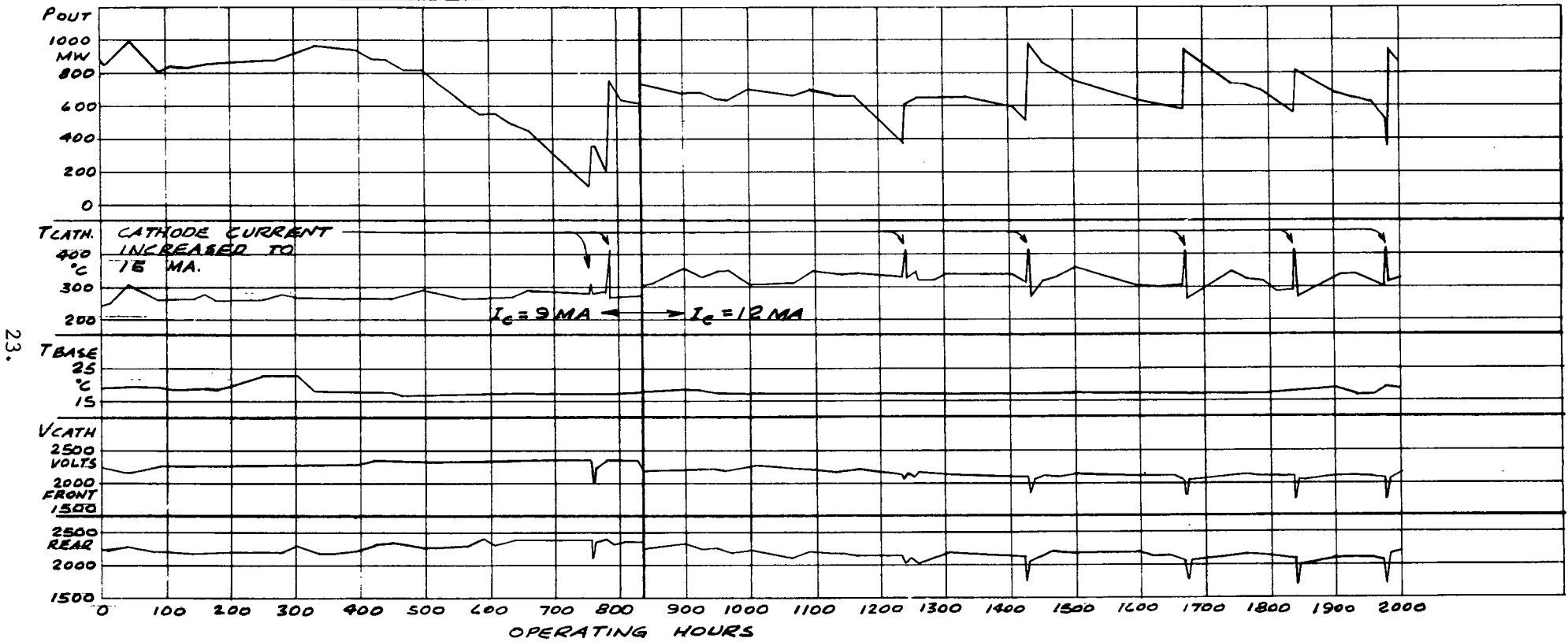
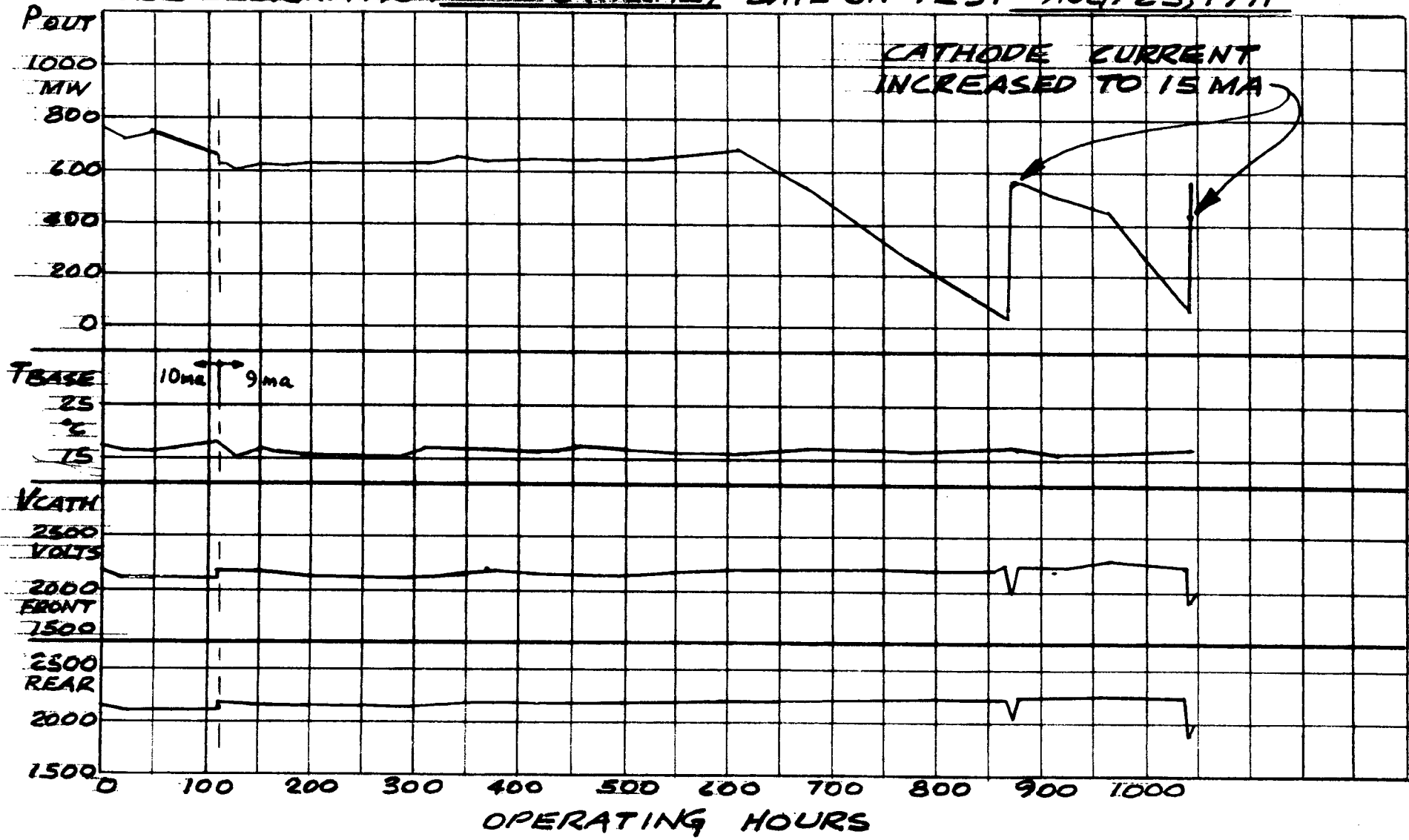


Figure 8 Life test results on standard tube (MC-STD-6)

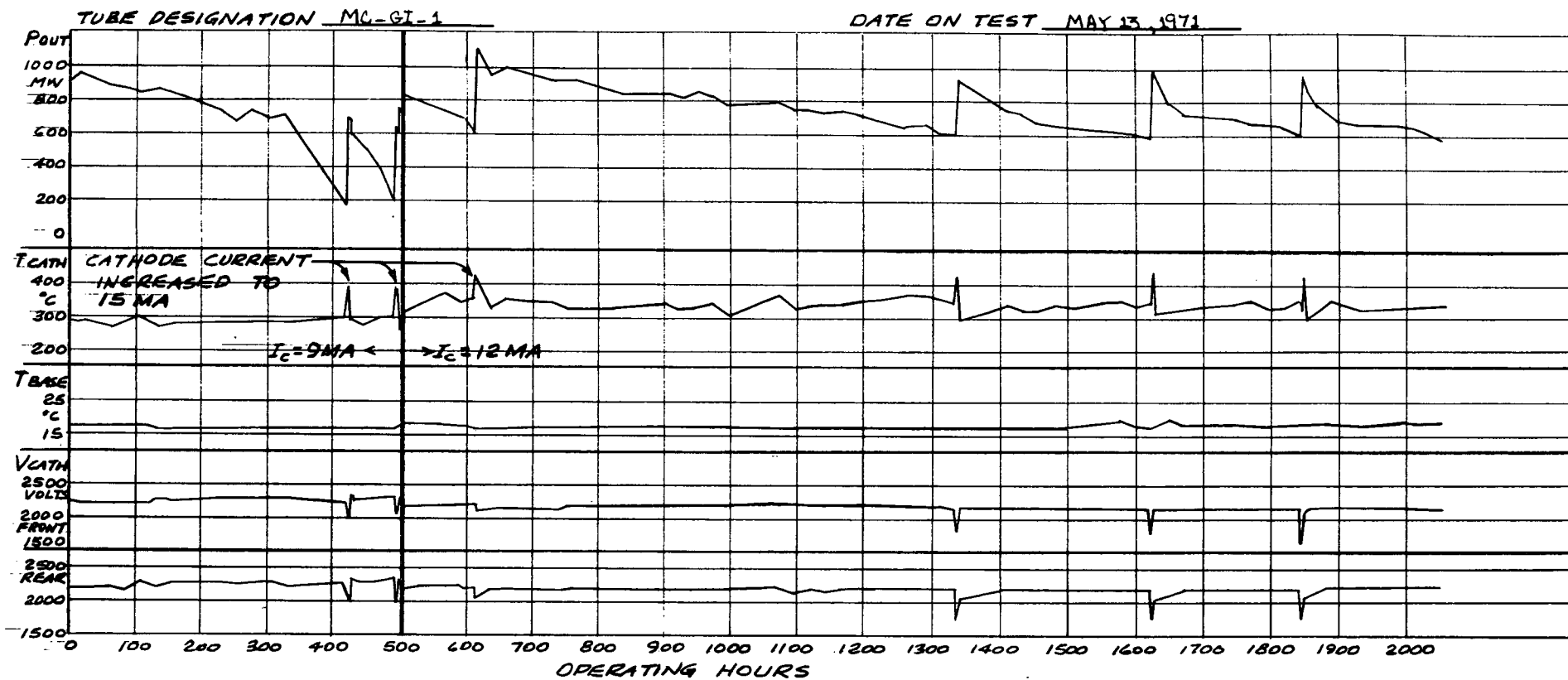
TUBE DESIGNATION MC-STD-8 (50% CO₂ OVERFILL) DATE ON TEST AUG. 25, 1971



25.

Figure 10 Life test results for tube with 50% overfill of CO₂ (MC-STD-8)

Figure 11 Life test results for tube with glass insert (MC-GI-1)



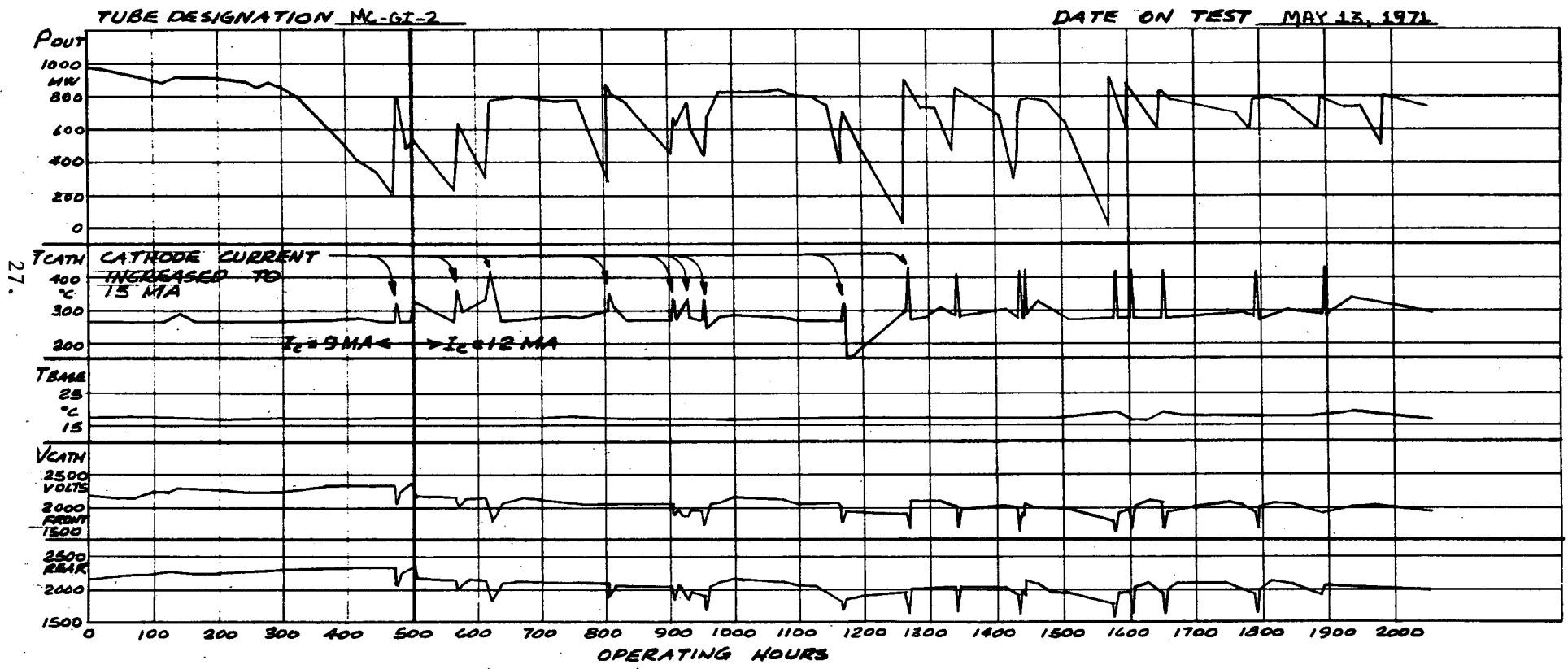


Figure 12 Life test results for tube with glass insert (MC-GI-2)

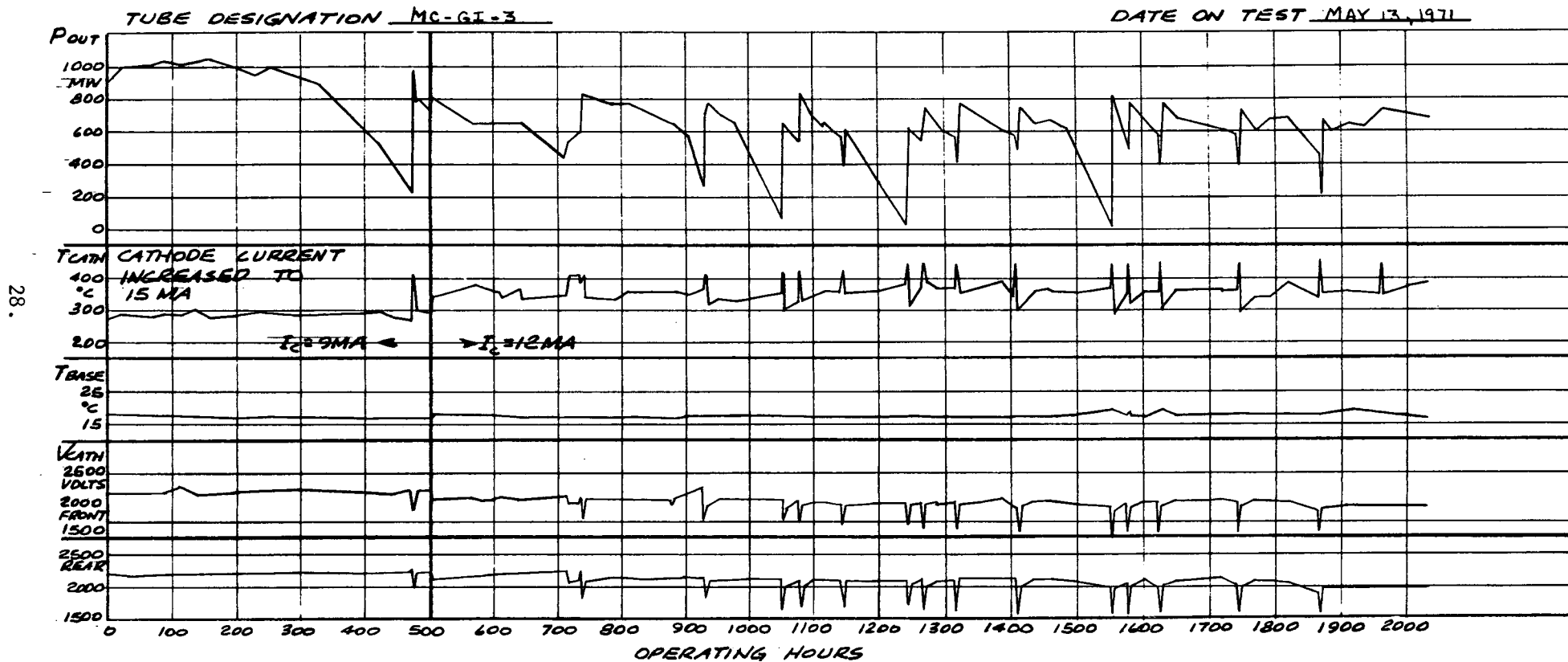


Figure 13 Life test results for tube with glass insert (MC-GI-3)

TUBE DESIGNATION MC-B-1

DATE ON TEST JULY 22, 1971

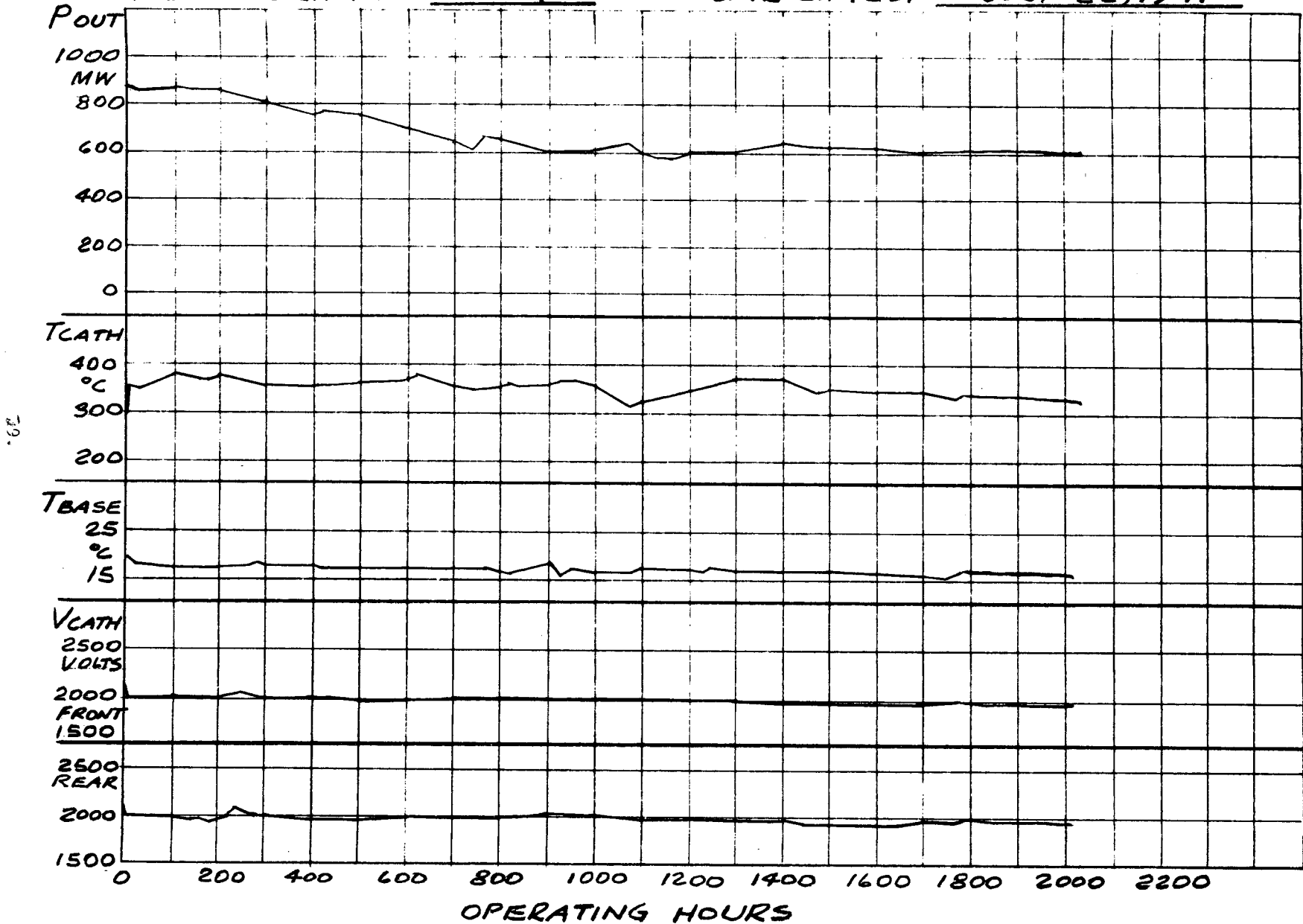
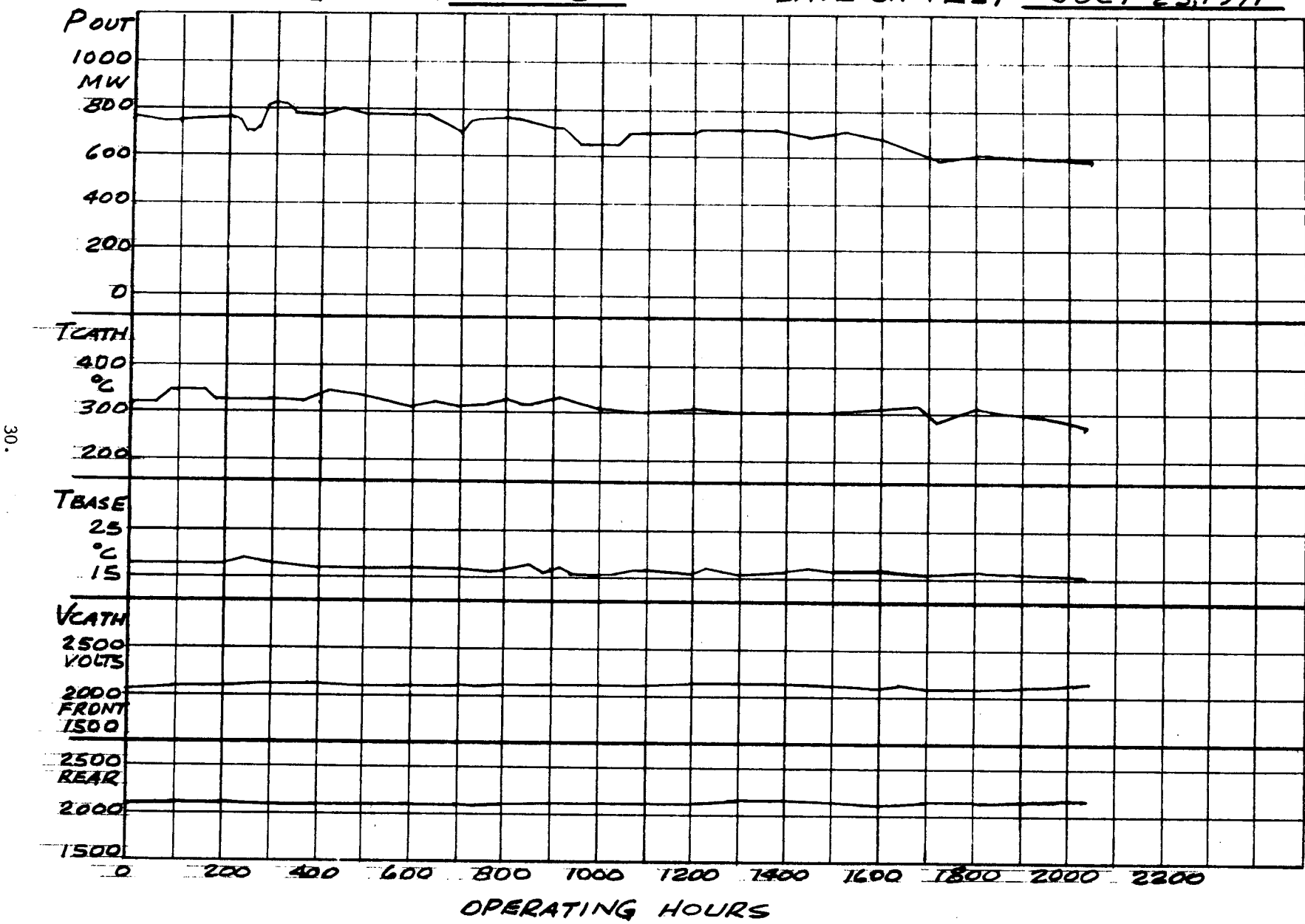


Figure 14 Life test results on tube with ballast tank (MC-B-1)

Figure 15 Life test results on tube with ballast tank (MC-B-2)

TUBE DESIGNATION MC-B-2

DATE ON TEST JULY 23, 1971



TUBE DESIGNATION R&D 1

DATE ON TEST 3/13/71

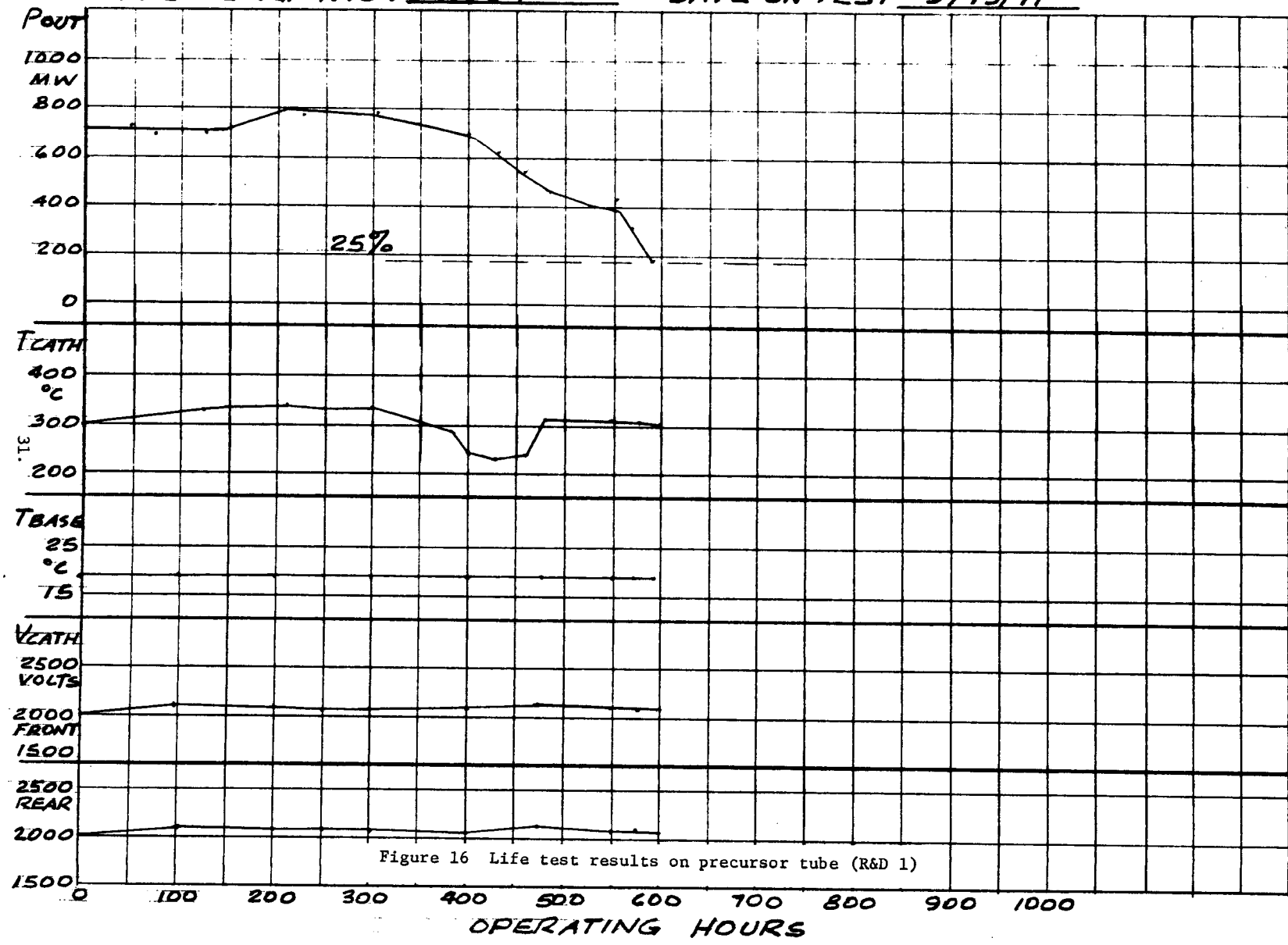


Figure 16 Life test results on precursor tube (R&D 1)

2.4 FAILURE ANALYSIS

2.4.1 Introduction

A failure analysis was performed on each of the tubes which had reached a power level less than 25% of its original power during the life test program. Although 8 of the 10 tubes life tested were run for at least 2000 hours, 6 of these had dropped to the failure level much earlier. The rejuvenation process applied to these tubes was considered to be an important part of their failure analysis. Although the main objective of the program was not to do extensive work in studying the life limiting factors in CO₂ lasers, some valuable information has been obtained from the limited post-failure efforts which is applicable for metal-ceramic lasers using pure nickel cathodes.

In order to obtain the maximum amount of information, a logical sequence of steps for analyzing the tubes was employed. As earlier tubes reached their failure point, the following examinations and tests were performed:

- 1) Tube rejuvenation
- 2) Analysis of tube gases
- 3) Refilling of the tube with a fresh mix and comparing its operation with operation at the start of life test.
- 4) Inspection of the tube exterior - especially the Brewster windows.
- 5) Thorough leak check of the tube.
- 6) Inspection of the tube's internal parts including absorption measurements on the Brewster windows.
- 7) Chemical analysis on cathode deposits.

The results of these tests, although not conclusive, were consistent from tube to tube, indicating the adequacy of the process controls. Because of the consistency of the results obtained on earlier tubes, additional tests were devised and performed on later tubes involving adsorption - desorption measurements, additional chemical tests, and further RGA analysis in order to more fully understand the failure process.

The analysis indicated that the tube failures were the result of fundamental processes rather than from random or controllable effects such as gas contamination from poor processing, inadequate cleanliness during tube fabrication, or leaks.

The following sections describe in more detail the examinations and tests performed during the failure analysis, and their results. Based on the relatively consistent results, a failure hypothesis is offered which appears to correlate the life time data obtained on tubes tested on this program, as well as data from several tubes tested on earlier efforts.

2.4.2 Residual Gas Analysis

The relative partial pressures of the tube gases were measured with the aid of an EAI Quadrupole Residual Gas Analyzer. To obtain good quantitative data it is required that the analyzer be accurately calibrated for each gas species before absolute partial pressures can be obtained. Over the relatively large pressure ranges of study here, we found that not only did the calibration vary with the pressure of each gas, but also with the mixture. Calibration for one condition can yield errors as high as a factor of 3 for another condition, therefore, calibration of the test equipment and reduction of the data has required a knowledge of the rate of change of the system calibration as a function of partial pressures of the tube gases.

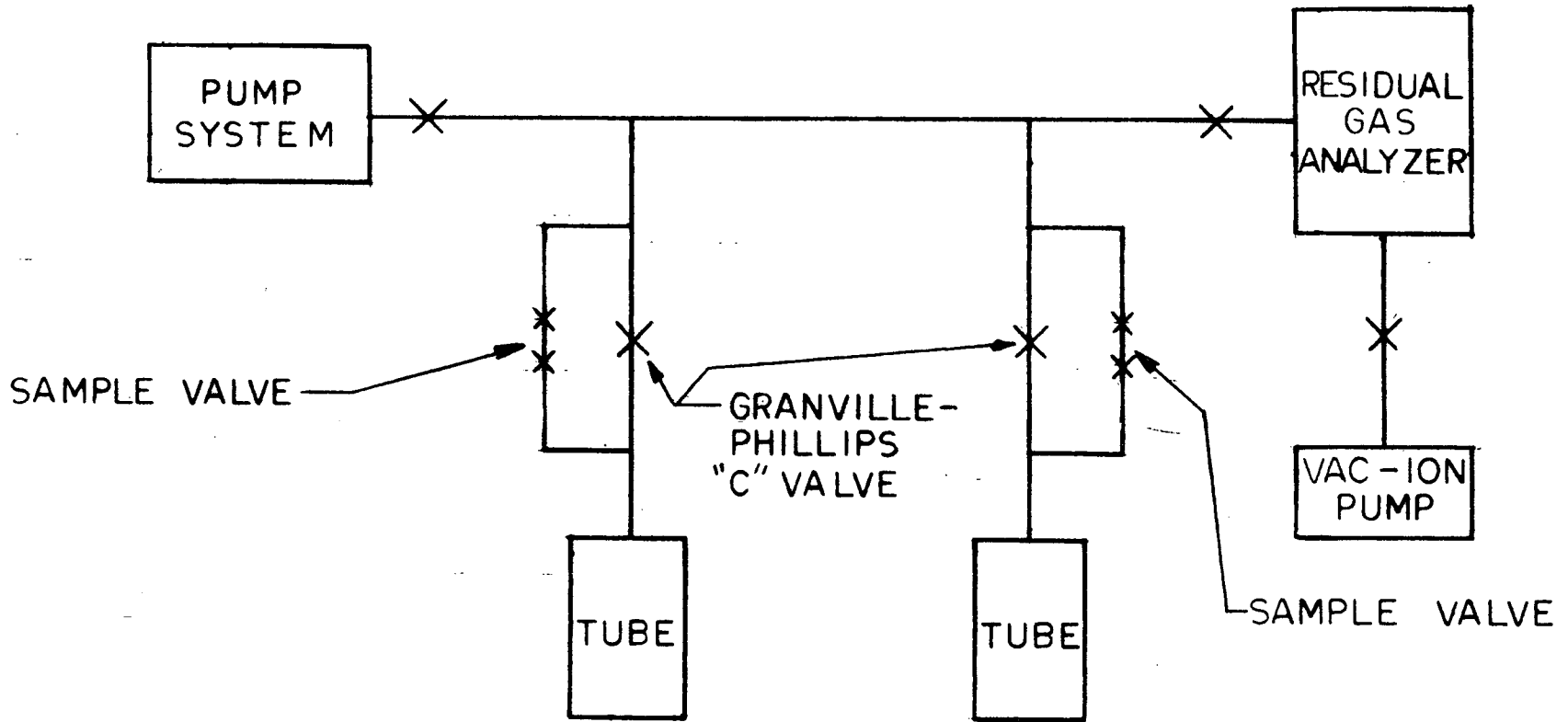
Also, since several of the gas components to be analyzed are composed of weakly bound molecules, the ionization current in the RGA tends to break down some of the gas species during the analysis period. As a result, a rigid timing procedure was required throughout the period of gas sampling, introduction of the gas sample into the RGA, and rate of scan of the RGA. Even with all of these precautions, it is expected that the absolute pressures which were derived are accurate only to within 20%. For the case of nitrogen and carbon monoxide, which share the same charge-to-mass ratio (28) in the RGA, it is difficult to measure their contributions separately. However, because of a markedly different RGA sensitivity figure between the two gases, techniques were developed which provided about 40% accuracy in the measurements of CO partial pressures.

As an aid in conversion from relative pressures to absolute pressures we have often used the helium gas from the laser mixture as a reference in RGA readings. Since this gas is chemically inert and is sputter-pumped relatively slowly, its partial pressure remains quite constant as a tube is operated for a long period of time. By using helium as a reference, changes in RGA configurations which may change the absolute peak heights as read from the RGA could be tracked out allowing absolute pressures to be calculated based on a known original fill pressure of helium.

Figure 17 is a block diagram of the gas analysis system. The gases are sampled from a tube of interest using a specially designed sampling valve obtained from Varian Associates. This solenoid actuated, gold O-ring sealed, all-metal valve, shown in Figure 18, withdraws a 0.1 cc volume of gas from the tube and deposits it in a gas manifold leading to the RGA. The RGA is evacuated to 10^{-8} torr prior to introducing the manifold gas. It is then operated statically between 10^{-4} and 10^{-5} torr during the analysis period. The gas is then removed by the RGA Ion pump system in preparation for the next sample.

To analyze the gases from the tubes which had failed, the tube was attached to the vacuum processing station by epoxying a glass tubulation over the break seal located at the tube center section. The sampling valve was attached in parallel with a 1/2 inch Granville-Phillips valve. All of the glass tubulation up to the break seal was evacuated to a pressure of less than 1×10^{-6} torr after which a magnet was used to manipulate a steel ball inside the tubulation to break the fragile breakseal. After waiting for several minutes for the gas mixture to come to equilibrium, samples were taken from the volume and analyzed. The mixture was analyzed several times in order to obtain an average which could be compared with gas analysis made on the initial fill prior to tip-off.

Table 3 shows the data obtained from the RGA analysis of several tubes at different periods of their life cycles. Under the column marked comments, the status of each tube just prior to the final RGA is given. The numbers given are average values of the absolute quantities of each particular gas. The RGA peak height ratios were changed to partial pressures using the appropriate RGA calibration factors for each gas. The "initial" readings



GAS ANALYSIS SYSTEM

FIGURE 17

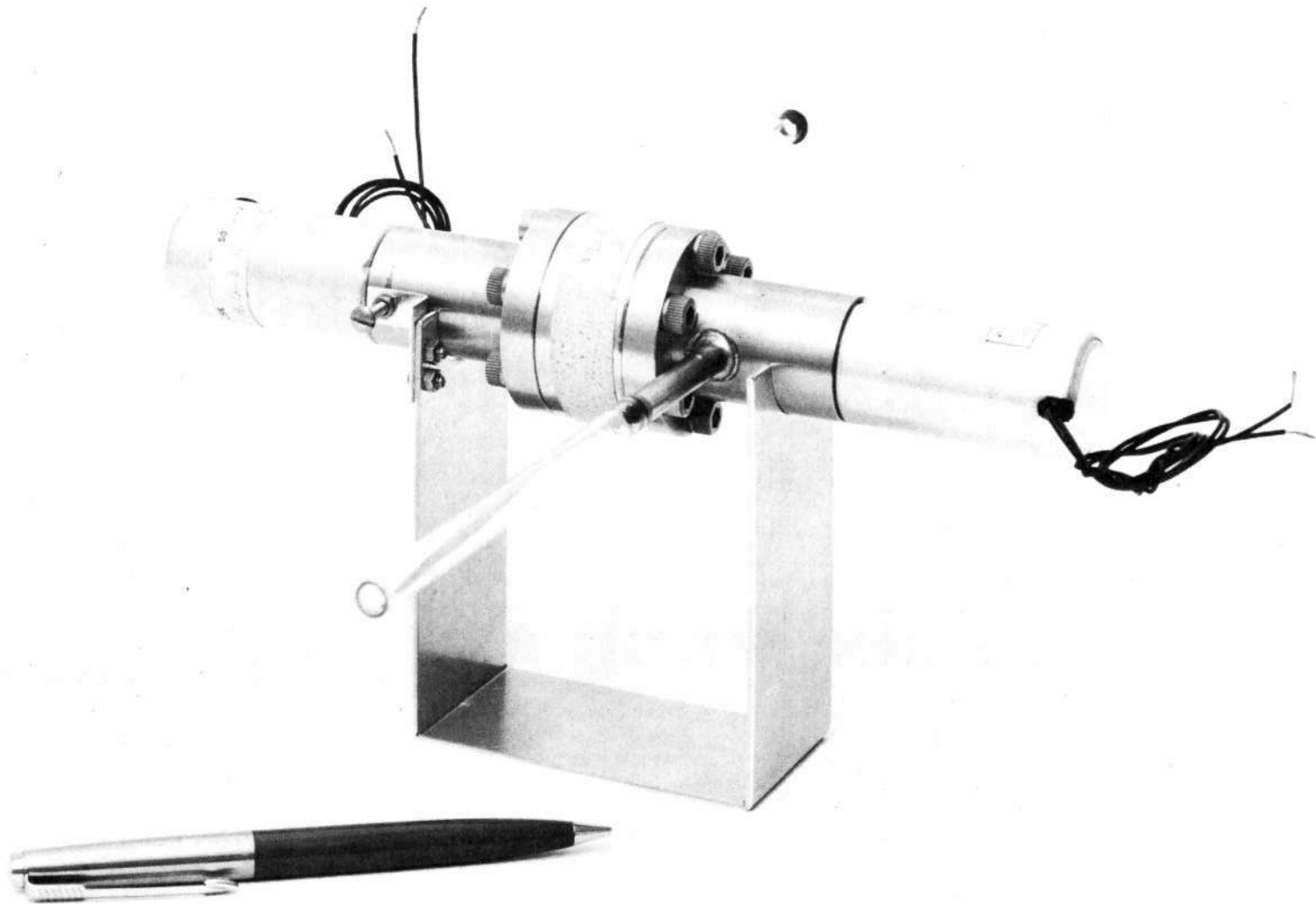


Figure 18. Photograph of Sampling Valve.

Table 3 - RGA Results for Life Test Tubes

		PARTIAL PRESSURE (TORR)											
Tube	Comments	H ₂			CO			O ₂			CO ₂		
		Initial	Tipoff	Final	Initial	Tipoff	Final	Initial	Tipoff	Final	Initial	Tipoff	Final
MC-STD-5	Final Power 650 mW. Two days from last re-juvenation	0.20	0.12	0.52	0.00	2.10	7.60	0.10	0.93	0.00	8.00	4.40	2.26
MC-STD-6	Final Power >800 mW completely re-juvenated just prior to RGA	0.20	0.12	0.24	0.00	2.10	1.90	0.10	0.93	0.10	8.00	4.40	4.70
MC-GI-1	Final Power 570 mW. Nine days from last rejuvenation	0.20	0.12	0.80	0.00	2.10	4.60	0.10	0.29	0.03	8.0	5.60	1.60
MC-GI-2	Let run until power equalled zero. Three days from last rejuvenation	0.20	0.12	0.12	0.00	2.10	1.45	0.10	0.29	0.00	8.0	5.60	0.47
MC-GI-3	Final power 660 mW. Three days from last rejuvenation	0.20	0.12	1.12	0.00	2.10	6.70	0.10	0.29	0.00	8.0	5.60	2.54

correspond to a time prior to initiation of the discharge, the "tip-off" values correspond to readings taken within the processing period (75-100 hours) prior to removing the tubes from the processing station. These readings were taken after the first 30 minutes of discharge, the time required to reach the initial dissociation equilibrium on the final mix. The "final" results were obtained after the tubes had failed, been rejuvenated and operated for at least 2000 hours, and were taken during their failure analysis.

Several trends can be identified upon inspection of Table 3. First, except for the case of MC-GI-2 which was run until its power dropped to zero, the glass-insert tubes showed much more residual hydrogen than the standard tubes. Although water vapor could not be measured specifically because of high background, the increased amounts of hydrogen in these tubes could imply substantial amounts of water vapor. The results show that at tip-off the glass-insert tubes had more CO_2 and less O_2 than the standard tubes, which seems to support the theories regarding the beneficial effects of H_2O vapor on reducing the dissociation rate of CO_2 . However, the glass insert tubes did not have increased lifetimes because of the slower dissociation rate.

In all cases the final amount of hydrogen was larger than the initial amount. The metal-ceramic tubes appear to act as a source of hydrogen throughout their lifetime. This is not surprising since numerous hydrogen brazes were performed on various tube components during their fabrication. Again for hydrogen, typical high background levels tend to make the numbers less accurate than for the other gases. Based on previous gas mixture tests, it is known that hydrogen partial pressures greater than about 0.5 Torr will quench laser action in the tubes. Thus the 1.12 Torr and 0.8 Torr measured on MC-GI-3 and MC-GI-1 respectively, is suspect since the output power from these tubes was near the initial power (after rejuvenation).

Second, during the initial breakin period, the amount of CO_2 decreased due to dissociation in the discharge, and the amount of H_2 decreased. We believe that H_2 decreased due to the formation of water-vapor upon combining with free-oxygen in the discharge. The amounts of CO and O_2 both increased as expected due to the dissociation of CO_2 .

Third, it appears that the amount of CO present in the tubes increases rapidly after the tube is operated subsequent to a rejuvenation cycle. In the case of MC-GI-2, which had been run until zero power output was obtained, a substantial amount of CO was apparently also consumed.

Fourth, only two tubes showed small amounts of oxygen present in their final gas analysis. They were MC-GI-1 and MC-STD-6. MC-STD-6 had just been rejuvenated prior to its final RGA, indicating that some oxygen was formed in the process. The second tube, MC-GI-1, had a history of requiring rejuvenation less frequently, which could be related to the fact that some oxygen remained. The final partial pressures of the gases of MC-STD-6, were very nearly the same as those obtained prior to tip-off, except that only a small amount of oxygen was detected.

No analyses were made on the remainder of the tubes as they had not failed at the writing of this report. Our conclusions based on this data will be presented in Section 2.4.5. See Section 2.4.4 for additional RGA tests.

2.4.3 Optical Tests

Three optical tests were run on various tubes to determine if Brewster window degradation was an important factor in their failure. First the external surfaces of the Brewster windows were examined under a Fizeau Interferometer to determine if the surface had somehow become distorted during the lifetime of the tube. The windows were found to be flat to less than one-fringe in the visible, exceeding their fabrication specification.

Several tubes were refilled with a fresh mix and operated to determine if optical losses of any kind existed in the tubes that were not present initially. On all tubes, for which this test was performed, the power output was down by an average of 30% from the pre-tip-off value, indicating additional losses.

In order to determine if the inside of the Brewster windows had been contaminated, some Brewster window assemblies were removed from the tubes and tested for transmission. It was found that the window loss had increased from their initial value of about 0.1% to an average of 0.8%

which, to the accuracy of the measurements, accounts entirely for the observed drop in power of the refilled tubes. We believe that the additional loss is due to both anode and cathode material being deposited on the inside surfaces by sputtering. Visual examination of the anodes disclosed some discoloration as well as small amounts of grayish-white deposit. The ceramic bore had small amounts of sputtered material deposited on the inside surface as evidenced by a shiny purple tint. Initially the bores are roughened and white. The results of these measurements have been used to determine what the basic lifetime would be if the window contamination process were the only failure mechanism present. Assuming that the sputtering causes a linear reduction in window transmission with operating time, the tube losses would be sufficiently high within about 8000 hours to cause the tube to fail.

2.4.4 Chemical, Spectroscopic, and Related Tests

Prior to dismantling the tubes to examine their internal parts, they were leak checked and found to be leak tight using a Veeco helium leak detector with a sensitivity of better than 6×10^{-10} STD-cc/sec of helium. The precursor tube, MC-STD-5, MC-GI-2 and MC-GI-3 were dismantled and chemical tests were performed primarily on their cathodes. The overwhelming evidence pointed to their cathodes as the source of their failures. All of these tube's cathodes had large deposits of a greenish-black material, similar in color to various forms of NiO and NiCO₃, formed on their emission surfaces. These deposits extended about 0.125 inch into the quartz supports. Figure 19 is a photograph of the deposits formed in one of the cathodes. The deposits appeared to be formed in mounds and had some degree of crystallinity. The areas of the surface which were not covered by these mounds appeared to be covered with a black tenacious film. The mounds themselves were rather powdery in substance and could easily be scraped off with a metal probe.

Two sets of cathodes and supports were sent to Sloan Research Industries Incorporated for x-ray diffraction and emission spectrographic analysis. The emission spectrographic analysis was performed to identify any contaminant metallic-elements. Only nickel, silicon (from the quartz) and platinum were found in any quantity. The x-ray diffraction analysis, which can only detect the presence of crystalline compounds, revealed the presence of only NiO and a possible unidentified intermetallic. The latter



Figure 19. Photograph of a Nickel Cathode after 2,000 Hours of Operation.

was only a trace amount. No carbon compounds of nickel (Ni_3C , NiCO_3 , etc.) were detected. Neither method was capable of detecting the presence of amorphous carbon, therefore its presence or absence was not verified. The detailed methods used and results are contained in Sloan Reports 177090 and 171160, found in Appendix A of this report.

The approximate weight of the deposits was found by removing them from the cathode and quartz support surfaces by dissolving them in a solution of H_2SO_4 , HNO_3 , glacial acetic acid, and H_2O . This cleaning solution is recommended for the removal of oxides from nickel. (2) This acid solution can dissolve NiCO_3 and Ni as well as NiO but will not dissolve pure carbon or Ni_3C . The weight of the cathode and supports was accurately measured before and after removal of the deposits, and from these measurements the weight of deposits removed was determined to be approximately 28 mg. Although an accurate quantitative measurement was not made, a large portion of the deposits removed were undissolved. These were assumed to be amorphous carbon and perhaps Ni_3C . A second test was performed by placing a cathode in hot NH_4OH , which will dissolve NiO but not NiCO_3 , or pure Ni. The cathode was removed after 30 minutes with a relatively large percentage of the deposits undissolved. Agitation of the cathode with a magnetic stirrer had loosened some of the undissolved material which remained in the beaker. The NH_4OH was then evaporated, and the beaker was weighed and compared to its initial weight, determined previously. The amount of deposit removed in this test was 3 mg. This quantity, although slightly high because of loosened undissolved particles is on the order of what one would expect if about one-half of the oxygen formed by dissociation of CO_2 (approximately 4 Torr in 150 cc volume) were combined with Ni to form NiO. (See Section 2.4.5.)

In order to understand the rejuvenation process more clearly, one cathode and quartz support from a tube which had failed were sealed in a glass vacuum tube with a thermocouple to monitor their temperature. The tube was attached to a sampling valve so that residual gas analysis could be performed on the gases given off upon heating. The test device is shown in Figure 20. The tube had a clear window so that changes in color or character could be observed as the temperature of the cathode, controlled by an external RF-induction coil, was increased. Prior to heating, the tube was evacuated to less than 1×10^{-6} torr to remove atmospheric gases and reduce background.



Figure 20. Cathode RGA Tester.

The tube was then backfilled with 5 torr of helium which served as a reference for residual gas analysis. Then samples were taken from the tube and analyzed at 50°C temperature increments as measured with the thermocouple. Figure 21 is a graph of the RGA results obtained, showing how the gases are evolved during rejuvenation. Below 200°C very small amounts of gas were driven off. However, as the temperature was raised to 400°C large amounts of CO + N₂ and CO₂ were produced. The amount of O₂ and H₂ were below the detection threshold of about 10⁻² torr. The color of the deposits changed from light green and black to khaki at the higher temperatures. Because of the duration of the test, it was conducted on two separate days. The first day a maximum cathode temperature of 300°C was reached. An RGA run was made on that day after the tube had cooled down to room temperature. Results showed that readsorption occurred to some extent on cool-down. The next day's test was started with a second RGA at room temperature, then the cathode and support were raised to a temperature of 250°C where the test was resumed. At reaching 450°C, the maximum temperature attained by a tube cathode in the rejuvenation cycle, the heat was removed and a final run was made after cool-down. The last point was taken after the tube sat for three days at room temperature. As shown by this point, once again the gases were re-adsorbed with about 60% of their maximum amounts obtained during the test still remaining. At room temperature, the deposits returned to their original light green or black color.

In order to separate N₂ and CO, two curves are shown, assuming in one case that all of the evolved gas with mass number 28 was CO, and in the other that all of it was N₂. There is no way to distinguish the two in this case, as the cathode and supports had been exposed to the atmosphere and could very well have had large amounts of N₂ adsorbed on their surfaces.

Subsequent to this test a related test was run on MC-STD-6 after it had been refilled. As the tube was run the gas concentrations in the tube were monitored for several hours. The data showed that if the tube were turned off for several hours, the relative quantities of CO₂, CO, and O₂

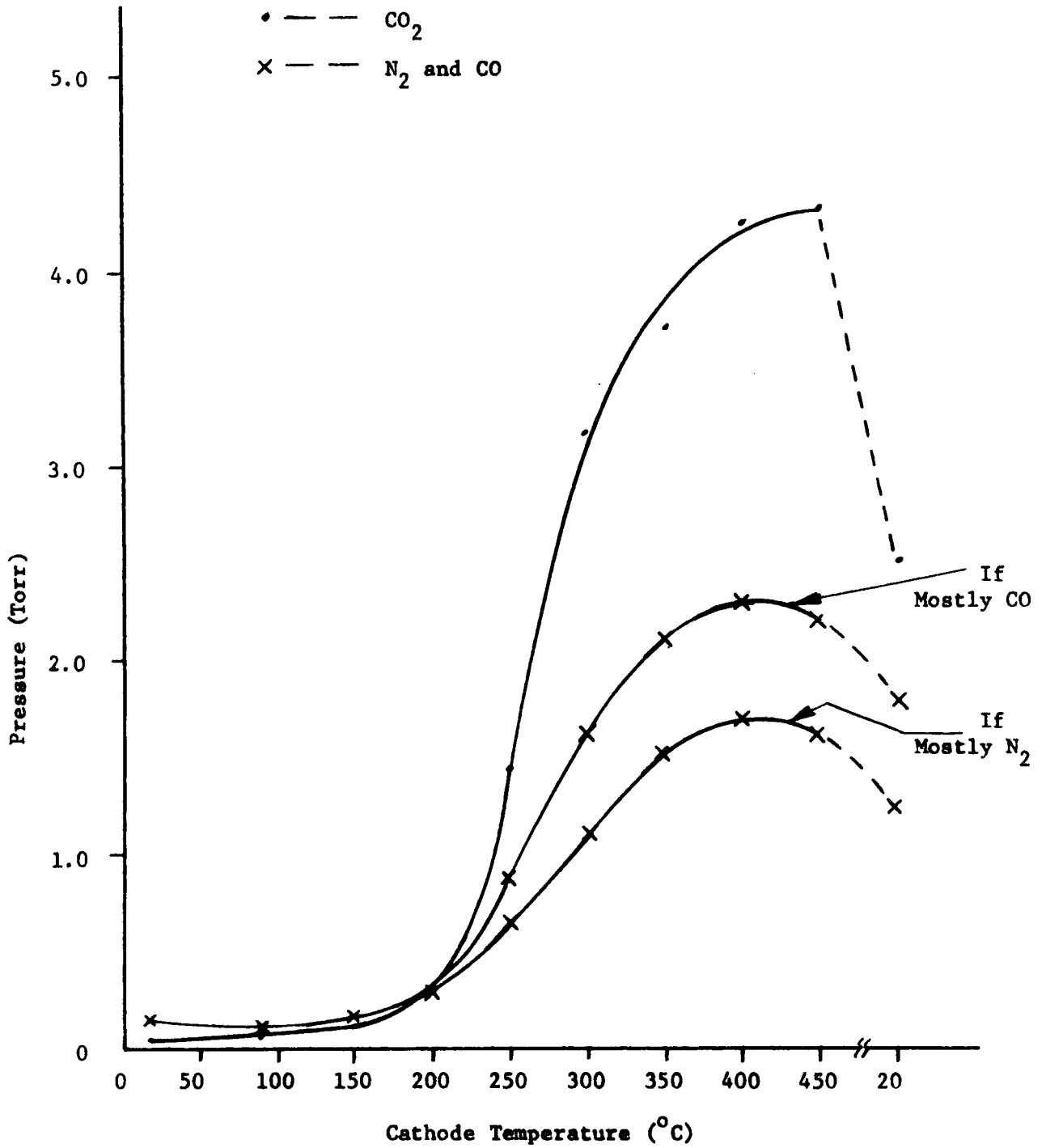


Figure 21. RGA Results of Desorption Measurements on Used Cathode.

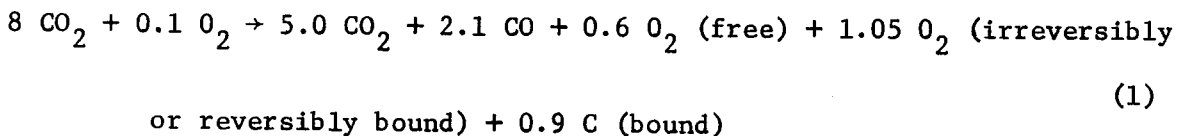
would decrease. The partial pressure of these gases would return when the tube was again turned on. The data also showed that the quantities of all of the gases were decreasing after about 10 hours of accumulated running time. Data obtained on an earlier program and the results obtained for the early stages of tube life on this program indicate that for a tube with a new cathode the relative quantity of O_2 increases for approximately 60 to 70 hours of operation and then starts to fall. The amount of CO rises and the CO_2 falls until the CO_2 is nearly consumed. Since this pattern was not followed for this test on MC-STD-6 it was concluded that physical adsorption and/or weak chemisorption were taking place on the cathode deposits and that the rates were much higher than for a clean cathode. The rapid gas clean-up rate and the fact that the reactions are reversible explains the periodic requirement for rejuvenation of MC-STD-6, and other tubes.

The proposed failure mechanism presented in the following section is based on the results obtained from these gas analysis studies and chemical tests. Although the hypothesis has not been proven, we believe that it satisfactorily explains the observed results.

2.4.5 Proposed Failure Mechanism

As has been shown by various gas analysis studies, the CO_2 of the laser mix disassociates in the discharge to form a quasi-equilibrium mixture of CO_2 , CO, and O_2 . Present results indicate the following condition is reached within the processing period for the tubes (~ 100 hours);

(Initial fill pressures) (Gas composition at tip-off)

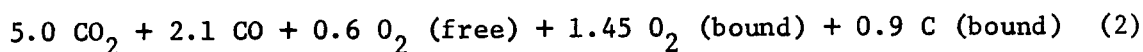


The $1.45 O_2$ and $0.9 C$ must be postulated in order to balance the equation. Since the oxidation of alpha-nickel is energetically favorable at the cathode temperature ($\sim 300^\circ C$)⁽³⁾, it is assumed that within the 100 hour operating period NiO has begun to form on the cathode emission surface.

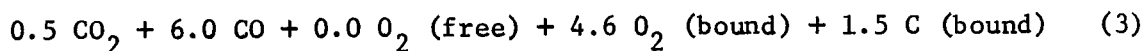
In addition, sputtered nickel deposited on the cathode and quartz supports may also be oxidized, and physical adsorption of oxygen on the nickel surface has most probably occurred.

The equation $5.0 \text{ CO}_2 \leftrightarrow 2.1 \text{ CO} + 0.6 \text{ O}_2$ is clearly not a stable equilibrium condition. The CO_2 dissociates further in an attempt to attain a stable equilibrium; however, this is not possible with an oxygen and carbon "sink" in the system. The dissociation process would normally continue until the cathode surface is covered with NiO, at which point further oxidation would occur at a much slower rate due to the protective property of NiO. However, as the formation of NiO continues, physical adsorption of oxygen, CO_2 and CO becomes the primary rate determining process. It has been observed that NiO strongly physically adsorbs these gases⁽⁴⁾. If there is a sufficient amount of CO_2 and hence O_2 present initially, the NiO formation and gas adsorption processes appear to saturate, with enough CO_2 and O_2 remaining to maintain a stable equilibrium. Thus, as demonstrated in the ballast tubes, tube life is not linearly proportional to tube volume.

If, as in the case of our standard fill and tube volume, there is insufficient CO_2 available, the reactions proceed with the disappearance of free oxygen, an increase in CO, and a corresponding decrease in CO_2 until most of it is consumed and the tube power output falls to zero. RGA results on gas mixtures of failed tubes indicate that the molecular composition changes from the tip-off values of

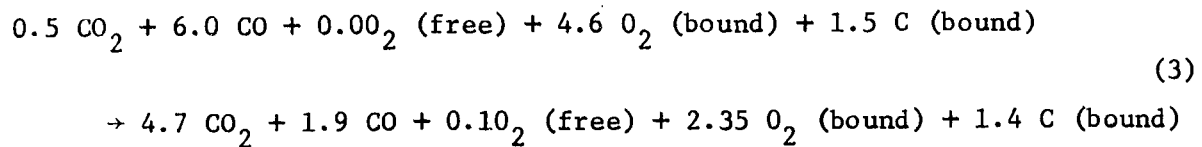


to that at failure of



Reference 4 indicates that CO can be adsorbed by NiO and catalytically oxidized by pre-adsorbed O_2 to form adsorbed CO_2 . In the rejuvenation process, described earlier, heating the cathode above 400°C drives off the catalytically formed CO_2 as well as reversibly bound O_2 . This now free O_2 becomes available for oxidation of the excess CO in the discharge, forming

more CO₂. In order to explain the complete recovery of the quantity of CO₂ present at tip-off, the following equation is proposed for the tube rejuvenation process;



The 2.35 torr O₂ which is not driven off during the rejuvenation process is most likely irreversibly bound as NiO, and the 1.4 C has most likely been consumed as pure amorphous carbon and Ni₃C.

In the well known Fischer-Tropsch Synthesis⁽⁵⁾, a commercial practice for producing higher order hydrocarbons, carbon-monoxide is catalytically oxidized in the presence of nickel, forming CO₂. In the process, reactions of the form $3\text{Ni} + 2\text{CO} \rightarrow \text{Ni}_3\text{C} + \text{CO}_2$ occur with Ni₃C as a by-product. It is believed that surface reactions of this sort with sputtered nickel contained in the NiO account for the irreversible removal of small amounts of carbon from the system. At the 300°C temperature of the cathode Ni₃C can be broken down to the elements. The insoluble deposits mentioned in Section 2.4.4 are most probably Ni₃C and pure carbon. The weight and volume occupied by these deposits could be quite high without noticing any great change in gas composition with the RGA, particularly if the quantity of helium in the tubes does not remain constant as assumed, but decreases slowly by sputter pumping or adsorption. To strengthen the above arguments more detailed measurements should be made on the residual carbon and nickel carbide remaining on the cathode and supports.

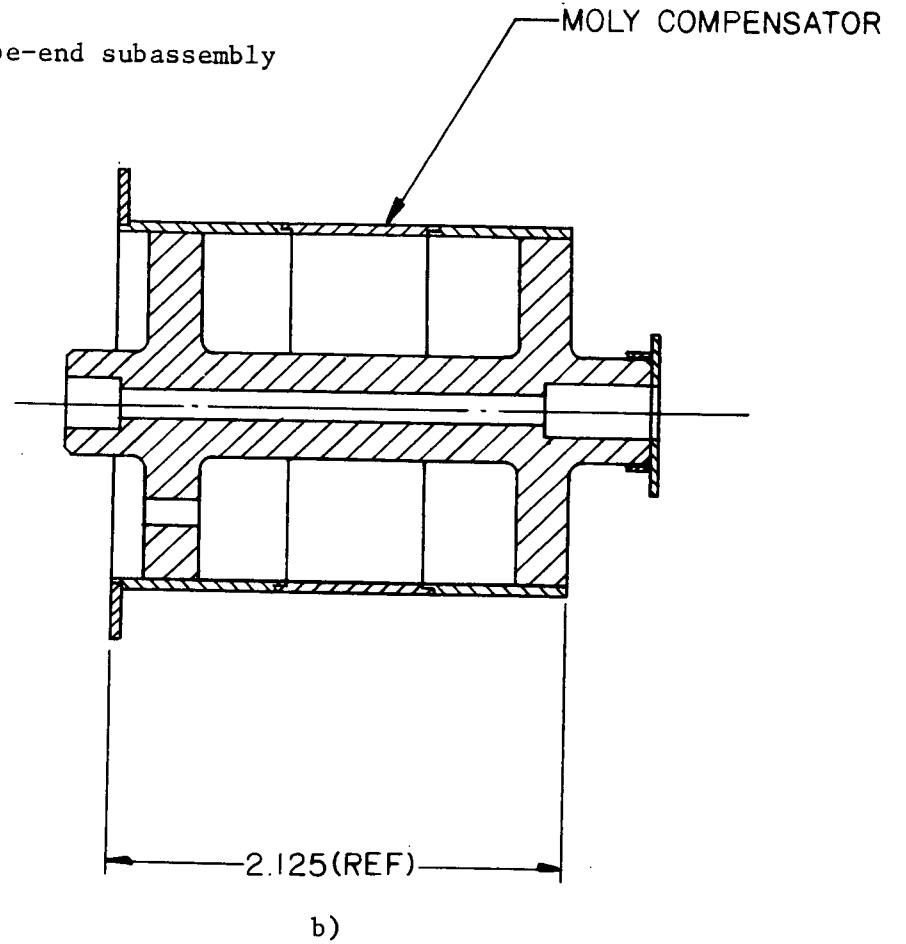
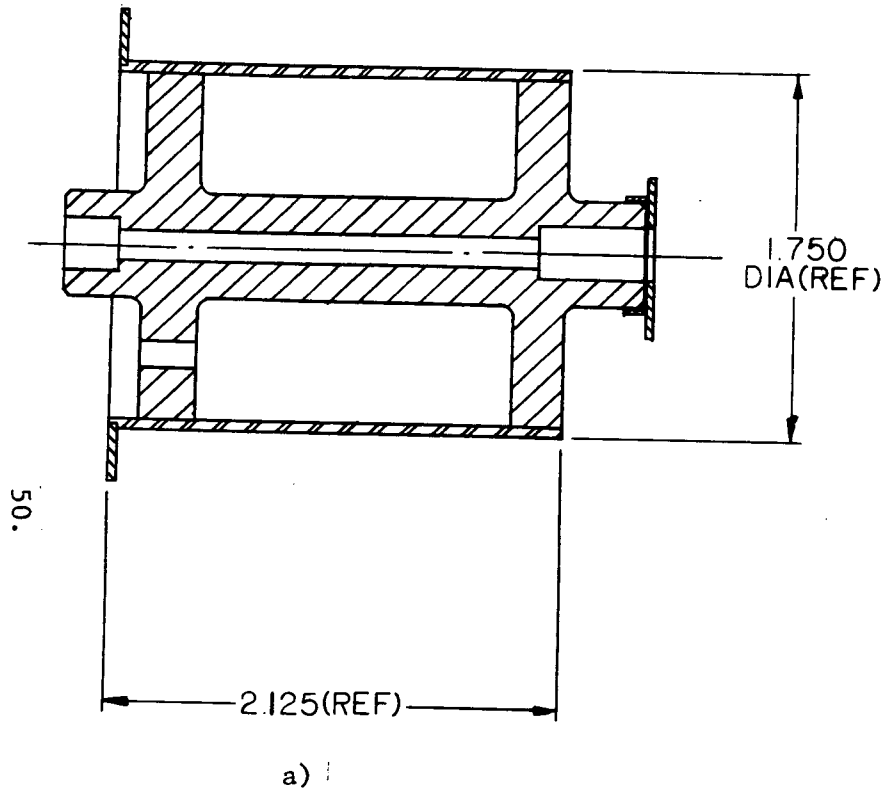
Three methods suggest themselves as possible methods for obtaining tube lifetimes in excess of 2000 hours for the case of tubes using nickel cathodes. (1) It may be possible to pre-oxidize and pre-process the cathodes so that the desired equilibrium state is reached early in the processing cycle of the tubes. Experiments would have to be performed to develop a suitable NiO surface, adherent enough, with good emission properties, and which would not sputter excessively for this to be a viable solution. (2) The initial rate of oxidation of the cathode could be lowered substantially

by reducing its temperature. This would extend the tube life by moving the point at which adsorption becomes the major gas clean-up mechanism far out into the tube's operating life. (3) Large gas-ballast can be added to the tubes. As was seen with the ballast tubes, the extra CO_2 provided in the larger volume allows the rapid chemical and physical reactions to saturate, with sufficient CO_2 remaining for the tube to continue lasing. This method of counteracting the failure mechanism, although effective, has two disadvantages. It adds additional weight and size to the standard tubes, and it does not prevent the formation of loosely adherent deposits which could scale off and be deposited on the Brewster windows in a weightless environment.

2.4.6 Metal-Ceramic Brazing Failures

As discussed in previous sections, a persistent leak problem occurred in the outer ceramic-to-ceramic braze joint during fabrication of several tube-end assemblies. After nearly a 100% yield on the first dozen subassemblies, the vendor's yield dropped to 10%. Many discussions were held with the vendor, going over all of the processes connected with this subassembly, in an attempt to determine the cause. It was initially believed that the outer Kovar shell was too stiff and did not yield during the cool-down cycle of the braze. Because of the expansion mismatch between BeO and Kovar at the braze temperature, it was expected that a large amount of shear stress could be in the ceramic-to-ceramic braze joint on cool down. It was believed that with the strength of the metallizing (9000 psi) this was a marginal situation even in good brazes. Subsequent tests, one using a molybdenum compensator ring in the outer Kovar shell (see Figure 22b) which allows the shell to more closely match the thermal expansion coefficient of BeO, and a second, performing an abbreviated assembly braze without any outer shell, proved that this was not the problem. Analysis made on the nature of the failures disclosed that tiny cracks were propagating under the metalizing layer indicating that the braze material itself was providing the force to pull the metalizing layer away from the ceramic. It was concluded that the initial metalizing batch, although it was properly mixed and controlled according to the vendor's process controls, was unusually strong

Figure 22 Metal-ceramic tube-end subassembly



and provided the margin for success. A second vendor, using pure copper as a malleable braze material and a different type of metalizing, was also unsuccessful. It became obvious that the assembly design had to be changed if we were to assure a reasonable yield.

The solution was obtained by eliminating the ceramic-to-ceramic braze altogether and forming the ceramic as a monolithic structure. This design provided several advantages.

- 1) The number of possible sources of leaks was reduced.
- 2) The amount of braze material exposed to the gases inside the tube was reduced.
- 3) The heat conduction capabilities of the assembly were increased by eliminating the ceramic-to-ceramic braze.

Figure 22a is a cross-section of the new tube-end assembly design. Two such assemblies were constructed according to the final design without any difficulties.

2.5 RELATED RESEARCH

2.5.1 Introduction

It was anticipated, and later verified, that the fundamental cause of failure of a sealed CO₂ laser tube is the gradual depletion of CO₂ within the tube. Although the mechanism responsible for this depletion are not yet wholly understood, a small effort on this program was directed toward circumventing the problem by either slowing the rate of CO₂ consumption or by providing the source of CO₂ within the tube to replenish that consumed. This section describes three sets of experiments performed along these lines.

According to Witteman⁽¹⁾, the addition of small amounts of H₂O vapor to the laser gas mix markedly increases the life of a CO₂ laser. One area of exploration was therefore aimed at slowing the rate of depletion of CO₂ by adding H₂O vapor to the tube. Experiments were performed wherein a

2

a molecular sieve material, Zeolite, saturated with water vapor was added to the interior of the laser tube. This material was to act as a reservoir of water vapor within the tube. If the conclusions drawn by Witteman were correct, the water vapor would catalyze the reformation of CO_2 from its dissociation products and effectively reduce the consumption rate of CO_2 .

A second set of experiments was performed which investigated the use of NiCO_3 as a possible direct source of CO_2 within the tube. Here, NiCO_3 within the tube would be heated to evolve CO_2 to replenish that consumed as the tube was operated.

One of the tubes used on this program had a glass center section to facilitate visual observation of its cathode. It happened that this laser was relatively long lived, possibly due to outgassing of H_2O by the glass. In case it was determined that the long life was indeed due to the glass, a third set of experiments was performed to vibrationally qualify the tube for the space craft environment.

2.5.2 Zeolite as a Water Source

Experiments performed by Witteman⁽¹⁾ in 1967 indicated that the addition of H_2O vapor to a CO_2 laser gas mixture extended the life of the laser. He theorized that the OH radicals catalyze the reformation of CO_2 from its dissociation products, CO and O. Therefore, the addition of H_2O within the tube effectively reduces the rate of consumption of CO_2 .

Accepting the premise that H_2O vapor is beneficial to tube life, one must then deal with the problem of introducing and maintaining the correct amount of vapor in the tube. The problem is not a simple one in that it was determined that if the partial pressure of H_2O is much greater than 0.5 torr, the power output of the tube is seriously effected; if much less, any beneficial effects may be lost. Several methods of adding the small amount of vapor were considered.

Adding water vapor from an external source is unreliable since water tends to be sorbed in unpredictable amounts by the tubing connecting the external source and laser tube. Water vapor could also be introduced

by adding to the laser mix stoichiometric quantities of H_2 and O_2 and forming H_2O in the laser discharge. The problem here is that the equilibrium gas mix resulting from the various chemical reactions occurring among the many gas constituents present within the electrical discharge is difficult to predict in any quantitative manner. Slight variations in the gas mix, especially the addition of H_2 , O_2 , or H_2O strongly effect the power output obtainable. Also, as the tube ages, the water content of the tube may vary appreciably as H_2O is sorbed by the tube material or dissociated in the discharge.

A third technique, that selected, is to add a small amount of molecular sieve material to the interior of the tube, saturate this material with water, and then let it act as a water reservoir for the tube. The partial pressure of water vapor in the tube can then be varied by varying the temperature of the sieve material. The following paragraphs detail the concept.

Molecular sieves are crystalline metal aluminosilicates, a class of compounds known as zeolites, with the peculiar property that the molecular pores of any particular type of molecular sieve are precisely uniform in size and molecular dimensions. The size of the pores determines what molecules are absorbed by the zeolite and which molecules are rejected, hence, the name molecular sieve. In other words, if the correct sieve material is used, it should readily absorb H_2O , one of the smallest of all molecules, and reject all others larger than H_2O . Such a zeolite is Linde Type 3A molecular sieve with a pore size of 3 angstroms.

The amount of water vapor absorbed depends on the condition of the zeolite upon exposure to water vapor, its dryness, and on the temperature of the zeolite. In effect zeolite saturated with water vapor can act as a water reservoir with the vapor pressure of water above it determined by its temperature. With saturated zeolite in the tube, any decrease in water vapor pressure due to chemisorption or decomposition will, to a large extent, be compensated for by a corresponding outgassing of the zeolite. The equilibrium water pressure can then be varied by changing the zeolite temperature. The following paragraphs quantitatively describe the situation by determining the change of H_2O partial pressure within the tube resulting from a given

change in the amount of water vapor due to processes not related to the presence of the zeolite.

The water vapor partial pressure in the tube, P, is given in terms of the gas temperature, T, and tube volume, V, by the expression

$$P = \frac{NkT}{V}$$

where N is the number of water molecules and k is Boltzman's constant. Since $N = \frac{M_{wt}}{m}$ where M_{wt} is the total mass of water vapor and m is the mass per water molecule given by the ratio of its molecular weight, 18, divided by Avogadro's number, 6.02×10^{23} , the pressure is given by

$$P = 3.46 \times 10^3 M_{wt} T/V \text{ torr}$$

where T is in $^{\circ}\text{K}$ and V is in cm^3 ($k = 1.036 \times 10^{-19} \text{ torr cm}^3/^{\circ}\text{K}$). Differentiating the expression for P with respect to M_{wt} and realizing that $dM_{wt} = -dM_{wz} - \Delta M$ where dM_{wz} is the change in water vapor mass retained by the zeolite and ΔM is the change in water vapor mass due to sorption or other processes within the tube that would occur if no zeolite were present one obtains

$$dP = -3.46 \times 10^3 \frac{T}{V} (dM_{wz} + \Delta M)$$

An expression for dM_{wz} , the change in water mass retained by the zeolite, must now be determined as a function of pressure and zeolite temperature.

Figure 23 shows the mass (gms) of water vapor, M_{wz} , sorbed by 100 gms of Linde Type 4A zeolite as a function of water vapor pressure for several zeolite temperatures, $T_z(^{\circ}\text{C})$. (According to Linde, Type 3A zeolite will sorb 87% of the water that Type 4A will sorb. This factor will be taken into account at the end of the analysis.) It can be seen that for the range of water vapor pressure between 0.1 and 0.5 torr, (the primary range of interest) these curves can be approximated by straight lines on this semi-log plot.

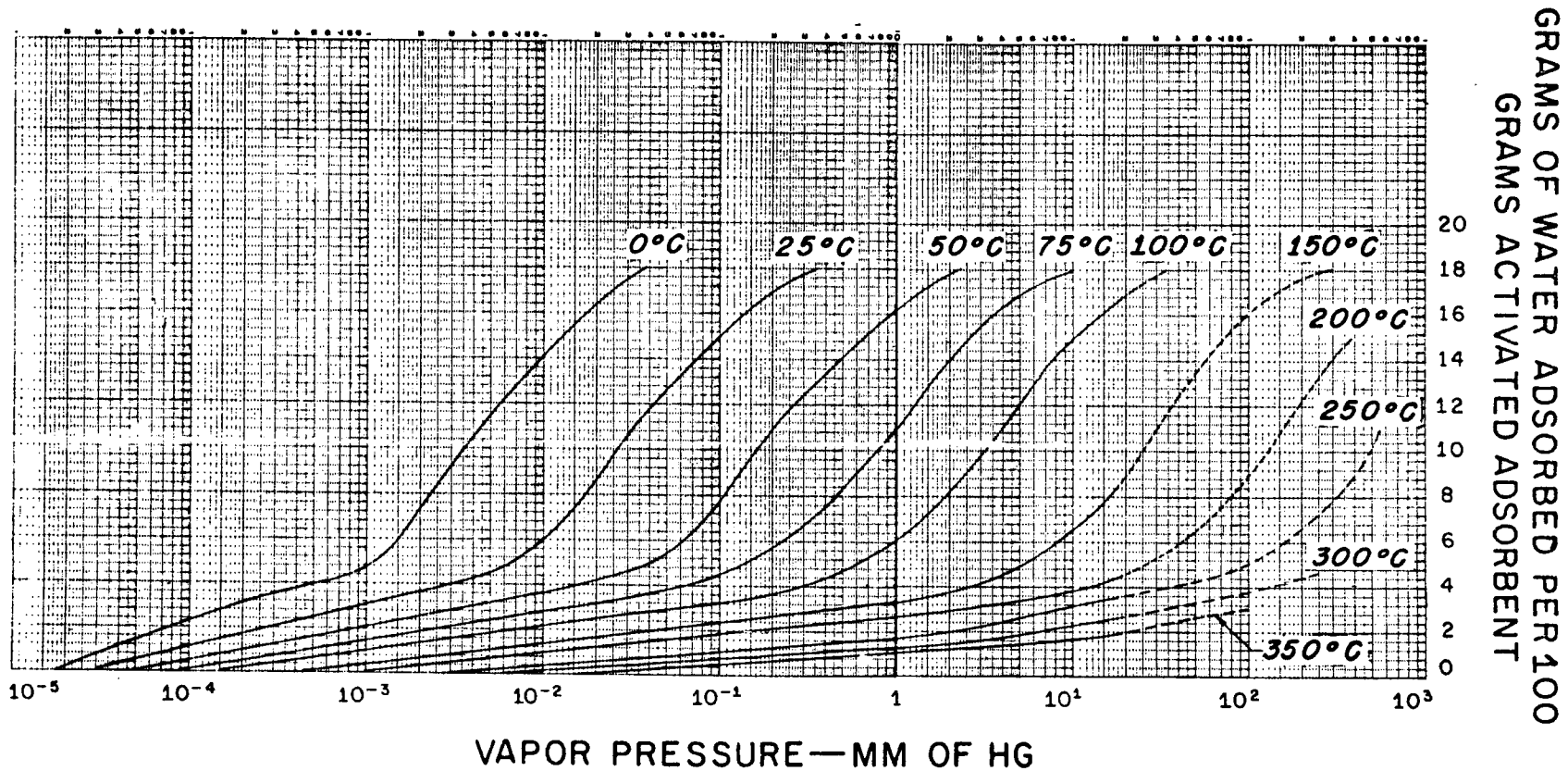


Figure 23 Water Vapor absorbed by Linde Type 4A Molecular Sieve vs. Vapor Pressure (from Linde Data Sheet No. 4A-1, 11-27-57).

Therefore, one can write

$$M_{wz} = \frac{M_z}{100} [A(T_z) + B(T_z) \log P] \text{ gms,}$$

where M_z is the mass of zeolite in gms. The intercept, $A(T_z)$, and slope, $B(T_z)$, and slope, $B(T_z)$, of the straight line fit are dependent on the temperature of the zeolite, T_z . Again referring to the curves in figure 22 these two parameters can be closely estimated by using the following empirical functions:

$$A(T_z) = \frac{A_2 e^{-C_2/T_z}}{T_z}$$

and

$$\log B(T_z) = \log A_1 - \frac{C_1}{T_z + D} \log e - B_1 \log (T_z + D) \quad \text{torr}$$

where A, B, C, and D are curve fitting parameters determined to be

$$\log A_1 = 40.0 \quad \text{torr}$$

$$B_1 = 16.5 \quad \text{torr}/\log^\circ\text{C}$$

$$A_2 = 6.49 \times 10^6$$

$$C_1 = 1600 \quad \text{torr } ^\circ\text{C}$$

$$B_2 = 7.83 \quad (\log ^\circ\text{C})^{-1}$$

$$D = 50 \quad ^\circ\text{C}$$

$$C_2 = 89.4 \quad ^\circ\text{C}$$

Differentiating the resulting expression for M_{wz} with respect to P and T_z , and substituting the result into the expression for dP obtained previously, one obtains the following expression for the resulting change in

pressure as a function of a zeolite temperature change, dT_z , and change in tube water content, ΔM :

$$dP = \frac{-\frac{kT}{V} \left\{ \frac{M_z}{100} \left[\left(\frac{C_2}{T_z} - B_2 \right) \frac{A(T_z)}{T_z} + \log P \left(\frac{C_1}{T_z+D} - B_1 \right) \frac{B(T_z)}{T_z+D} \right] dT_z - \Delta M \right\}}{\left[1 + \frac{kT}{100VP} M_z B(T_z) \log e \right]} \text{ torr}$$

where $K = 3.46 \times 10^3 \text{ cm}^{-3} \text{ torr gms}^{-1} \text{ }^\circ\text{K}^{-1}$.

The expression can be simplified if

$$M_z \gg \frac{100 VP}{KT B(T_z) \log e}$$

With this condition met, and recalling that $\Delta M = \frac{V\Delta P}{KT}$ where ΔP is the water vapor pressure change occurring if zeolite were not present, one obtains the expression

$$dP = \frac{\left[\left(-\frac{C_2}{T_z} - B_2 \right) \frac{A(T_z)}{T_z} + \log P \left(\frac{C_1}{T_z+D} - B_1 \right) \frac{B(T_z)}{T_z+D} \right] dT_z + \frac{100V \Delta P}{KT M_z}}{B(T_z) \log e/P} \text{ torr}$$

For a zeolite temperature, T_z , of 50°C , initial water vapor pressure of 0.5 torr , gas temperature of $25^\circ\text{C} = 298^\circ\text{K}$ and tube volume of 150 cm^3 , the resultant change in water vapor pressure is

$$dP = 0.0446 dT_z + 0.0019 \frac{\Delta P}{M_z} \text{ torr}$$

(With these parameters the simplified expression for dP can be used since

$$\frac{100 VP}{KT B(T_z) \log e} = 0.0019.)$$

Since Type 3A zeolite was to be used, M_{wz} should be reduced by a factor of 0.87. The final expression for dP for Type 3A zeolite is

$$dP = 0.0446 dT_z + 0.0022 \frac{\Delta P}{M_z} \text{ torr}$$

It can be seen that the change in water vapor pressure is relatively insensitive to water consumption or zeolite temperature fluctuations.

Based on these theoretical considerations, three laser tubes were designed to incorporate a small quantity (0.1 gm) of zeolite. The zeolite was contained in a copper oven attached as an appendage to the modified center section of a standard metal-ceramic laser tube. Figure 24 depicts the design of the laser tube and zeolite appendage.

The temperature of the copper oven containing the zeolite was maintained to within a fraction of a degree centigrade of a preset temperature by the combination of two 10 watt heater elements embedded in the copper, a temperature sensing thermistor also embedded in the copper, and external electronics. The current through the heaters was turned on or off by the electronics diagrammed in Figure 25 according to the temperature sensed by the thermistor.

Although the ovens and their associated electronics were designed and fabricated, a change in the program plan resulted in them not being used on any life test lasers. The program plan was changed partly due to results obtained with an experimental tube designed to test the zeolite addition concept. The following paragraphs describe these experiments.

A tube was fabricated with the basic metal-ceramic design modified to have a glass center section with an attached glass oven appendage containing the zeolite. Many experiments were performed to determine the effects of zeolite on the partial pressures of the various tube gases as a function of zeolite temperature. The partial pressure of tube gases was measured with a residual gas analyzer.

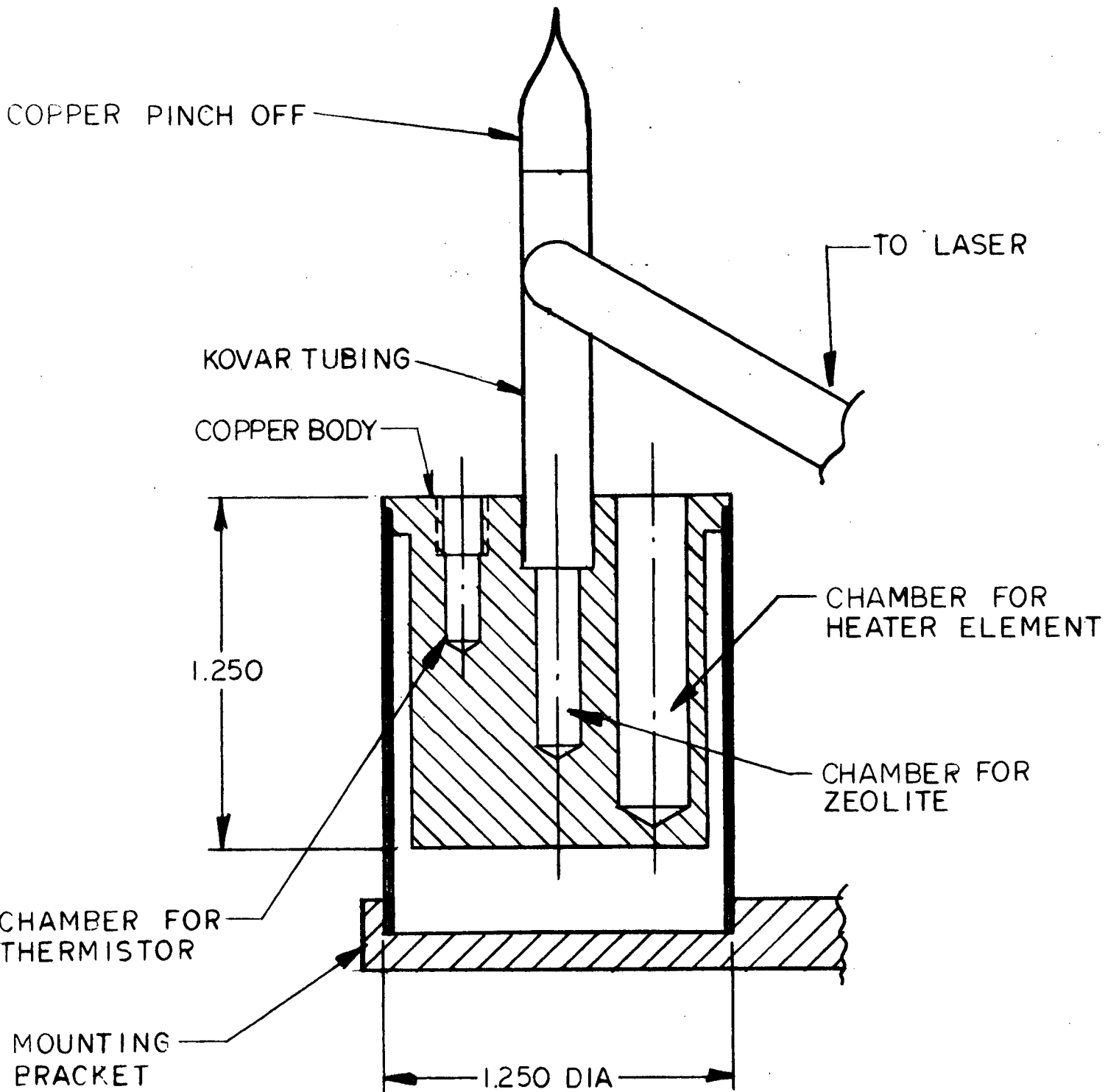
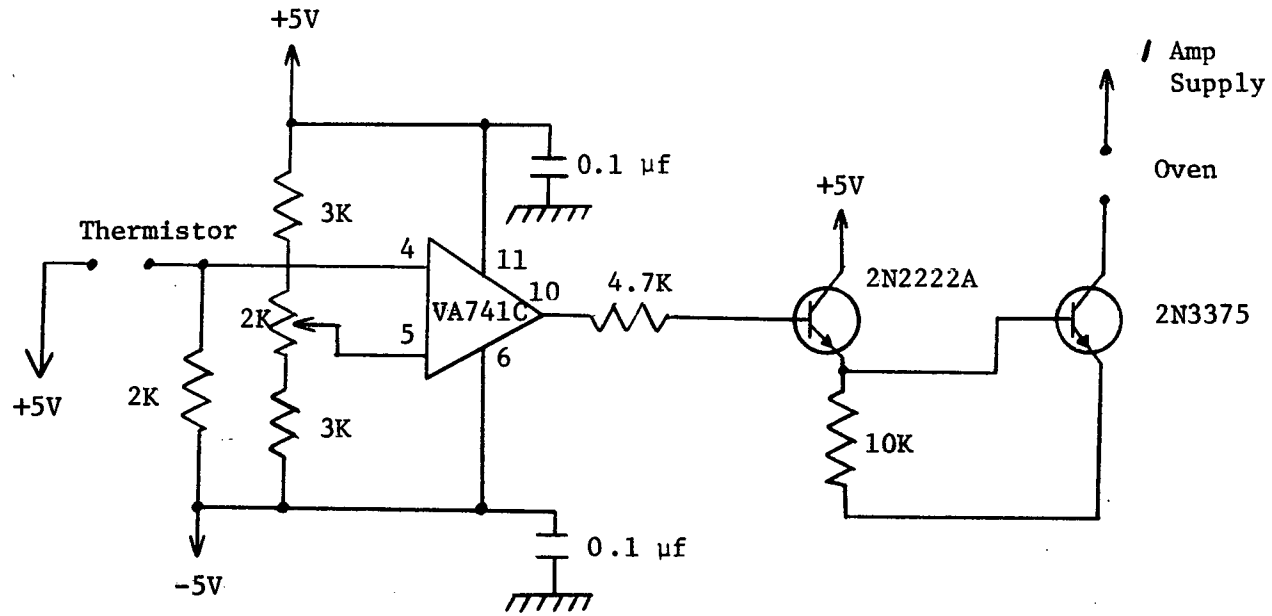


Figure 24 Zeolite Heater Assembly

Figure 25 Zeolite Oven Controller



It was found that the small pore size zeolite (Linde Type 3A) does not absorb a significant amount of H_2 , O_2 , He, CO_2 , N_2 , or CO for zeolite temperatures between 20 and $300^\circ C$. However, it can absorb large quantities of H_2O . According to the calculations given previously, 95 mg of zeolite should be capable of absorbing about 260 times the water vapor which would normally be obtained in a standard tube gas mixture. By operating the zeolite at a constant temperature of about $50^\circ C$, the partial pressure of the water vapor above the zeolite can be maintained at approximately 0.1 torr. The accuracy of zeolite temperature control required to maintain this partial pressure should be approximately one or two degrees, well within the range of the controller designed.

The most satisfactory technique for the introduction of an accurate amount of water vapor into a zeolite tube was found to involve the formation of water vapor in the tube from its constituents rather than directly adding water vapor. The procedure used with 95 mgms of zeolite called for the filling of a tube with 26 torr H_2 , 13 torr O_2 and 10 torr He. The tube was then discharged. After only 10 minutes of operation the hydrogen and oxygen was completely combined and absorbed by the zeolite as confirmed by residual gas analysis. Since the tube we were using for these experiments utilized a glass center section it was easy to observe the change in discharge color from a characteristic water vapor purple to pure helium pink. The tube voltage also dropped from about 220 volts to about 800 volts as the water vapor was absorbed by the Zeolite. Without the discharge present, the H_2 , O_2 , He gas mix did not measurably change with time (at least over several hours). After the Zeolite had been charged with water vapor, the helium was quickly exhausted so as not to pump out a significant amount of water vapor and the tube was filled with a standard laser mix.

The tube was then run for 480 hours to compare the variation of gas composition and tube voltage and power with those parameters of a standard tube. The all metal-ceramic tube that this Zeolite tube was compared with had also been used in many other experiments where it had been filled and evacuated many times. The life history of the Zeolite tube is shown in Figure 26. The two tubes were very similar in their life histories for the first 100 hours in that the power, CO_2 content, and O_2 content all

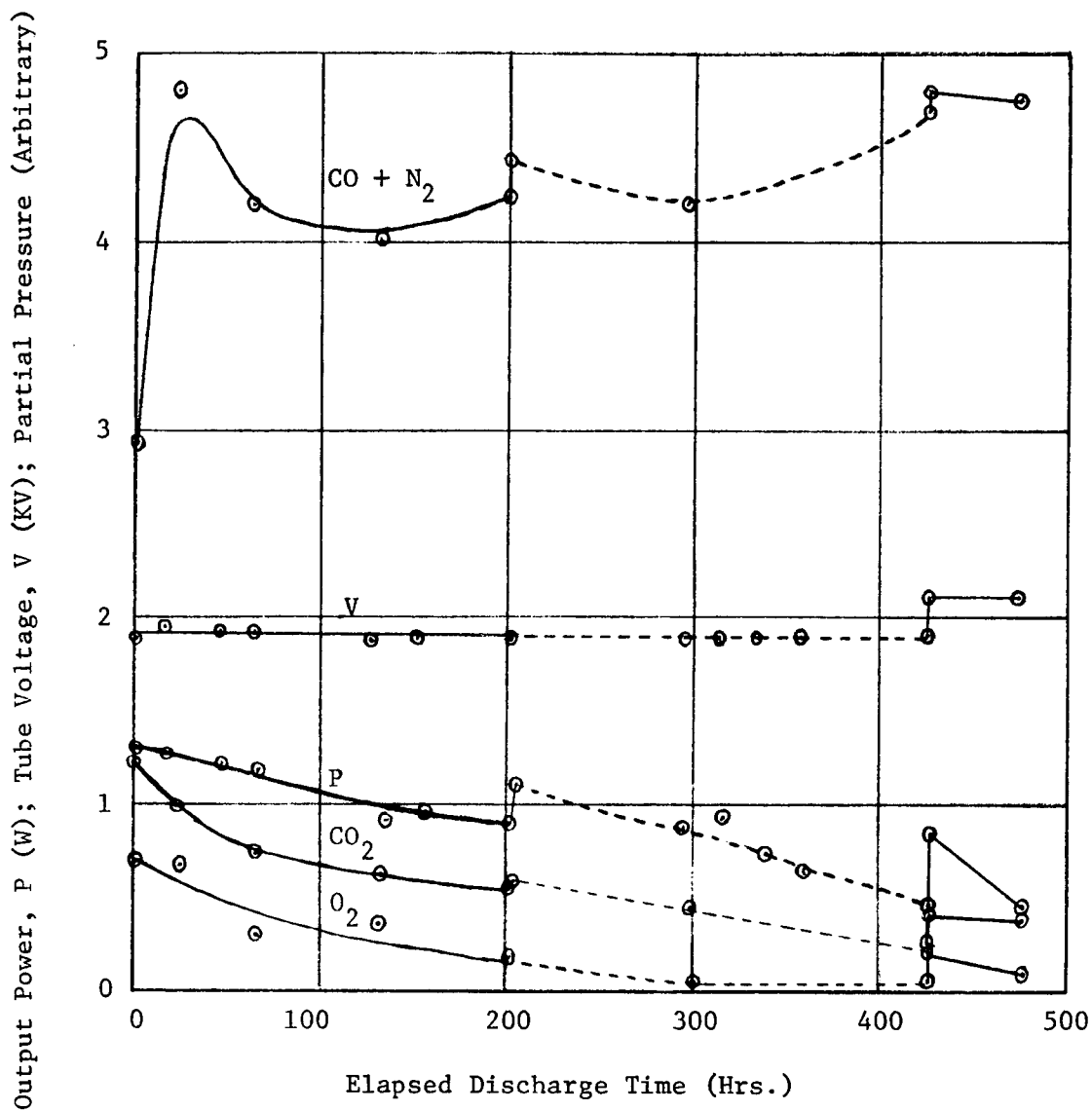


Figure 26 Zeolite Tube Parameters vs. Discharge Time.

Zeolite Temperature = 50°C corresponds to solid lines.
 Zeolite Temperature = 60°C corresponds to dashed lines.
 At 425 hours, Zeolite temperature was raised to 250°C
 and then lowered to 50°C.

decreased at approximately the same rate. From residual gas analysis and a leak check at the end of the 480 hour test, it was determined that the Zeolite tube started leaking after about 130 hours of discharge. At 200 hours it was noticed that the rate of decrease of power was slightly greater for the zeolite tube than for the standard tube. After raising the temperature of the zeolite to 60°C at the 200 hour mark, the power increased by 26%. The CO₂ and CO+N₂ content increased also.

The power and CO₂ content continued to decrease at the previous rate from this point as the tube was discharged an additional 225 hours. At 425 hours, the zeolite temperature was raised to 250°C and then returned to 50°C in a day's time with the discharge turned off. The result was to markedly increase the CO₂ partial pressure in the tube. The CO+N₂ and O₂ content also increased. This result indicated that the zeolite or its glass oven may absorb some gas over a long period of time. Upon discharging the tube, it was found to have increased in power from 450 mw to 810 mw, 65% of the initial power of 1.25W. Baking the zeolite had also increased the voltage from its previously constant value of 1900V to 2100V. This is indicative of a pressure increase.

In another 50 hours, the power had dropped back to the 450 mw level, but the voltage remained at 2100V and the CO₂ remained at the level it acquired just after bake. The test was terminated at this time after 480 hours. The power decrease could be caused by either the air leak or the CO₂ partial pressure decrease.

Time limitation forced this effort of the program to be concluded before extended life data could be obtained. Preliminary results indicated that the zeolite does indeed perform the function of a water reservoir. However, there is also some evidence that the zeolite may absorb some of the laser gas constituents. Further research must be performed before the merits of a zeolite addition to a CO₂ laser tube can be properly assessed.

2.5.3 Nickel Carbonate as a CO₂ Source

A more direct approach to solving the problem of maintaining a constant partial pressure of CO₂ within a sealed laser tube is to provide a source of CO₂ within the tube which would compensate for any CO₂ depletion.

One source considered was NiCO_3 which gives off CO_2 when its temperature is raised to about 300°C . To determine the possible effects of putting a temperature controlled sample of NiCO_3 in a laser tube, a small amount of NiCO_3 was put in a glass oven connected to the vacuum station, residual gas analyzer, and a capacitive manometer absolute pressure gauge.

The first thing noticed was that it was difficult to outgas the NiCO_3 powder; a pressure of 8μ was achieved after several days of pumping. It was found that H_2O vapor was the primary outgassing constituent.

Figure 27 shows the total gas pressure (in arbitrary units) as the oven temperature was increased. Note the rapid rise in pressure occurring when the NiCO_3 temperature was raised to about 300°C . The primary gases given off were CO_2 and CO .

It is not clear, then, that the use of NiCO_3 as a CO_2 source would not produce deleterious effects in a laser tube. The fact that the NiCO_3 was difficult to outgas shows that it may absorb some of the gases from the laser mix. Another deleterious effect is that one product evolved from the heated NiCO_3 was CO , a gas desired to be kept to a minimum within the laser tube.

2.5.4 Vibration Tests on Glass-Center-Section Tube

On an earlier program a metal-ceramic tube was constructed for use primarily in a Brewster window tester jig. This tube, shown in Figure 28, utilized a glass center-section epoxied to the standard BeO -kovar tube end sections. The glass center-section allowed visual observation of the discharge characteristics and the physical processes occurring in the region of the cathode during operation. The tube was processed extensively and was also filled with 50% extra CO_2 . It was decided early in the program that when the tube failed it should be subjected to a vibration test to determine if the glass as well as the epoxy joints could withstand liftoff environments. The tube was used in our Brewster window test fixture throughout the fabrication of all of the tubes on this program and failed near the end of the program after more than 5000 hours of operation.

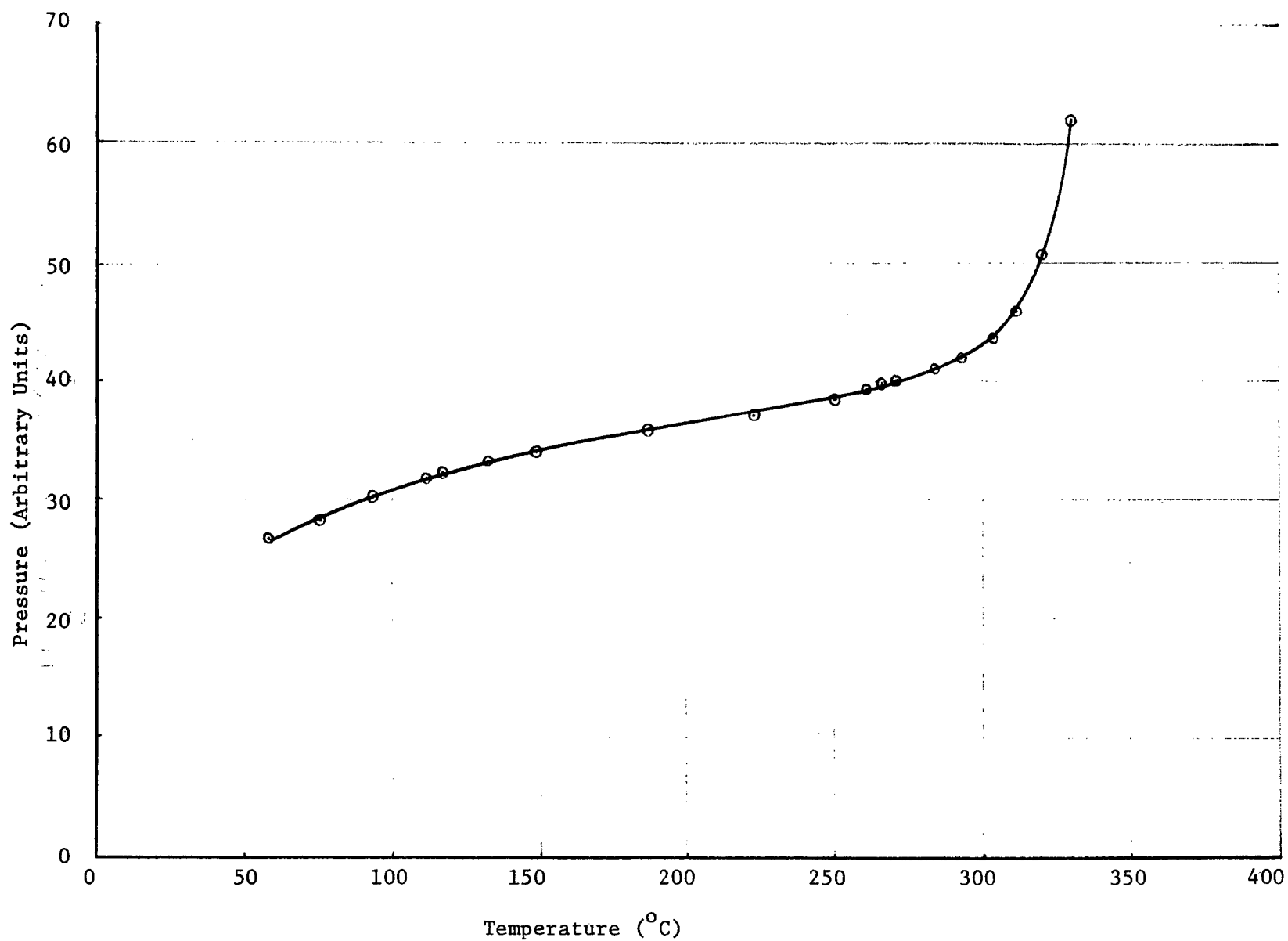
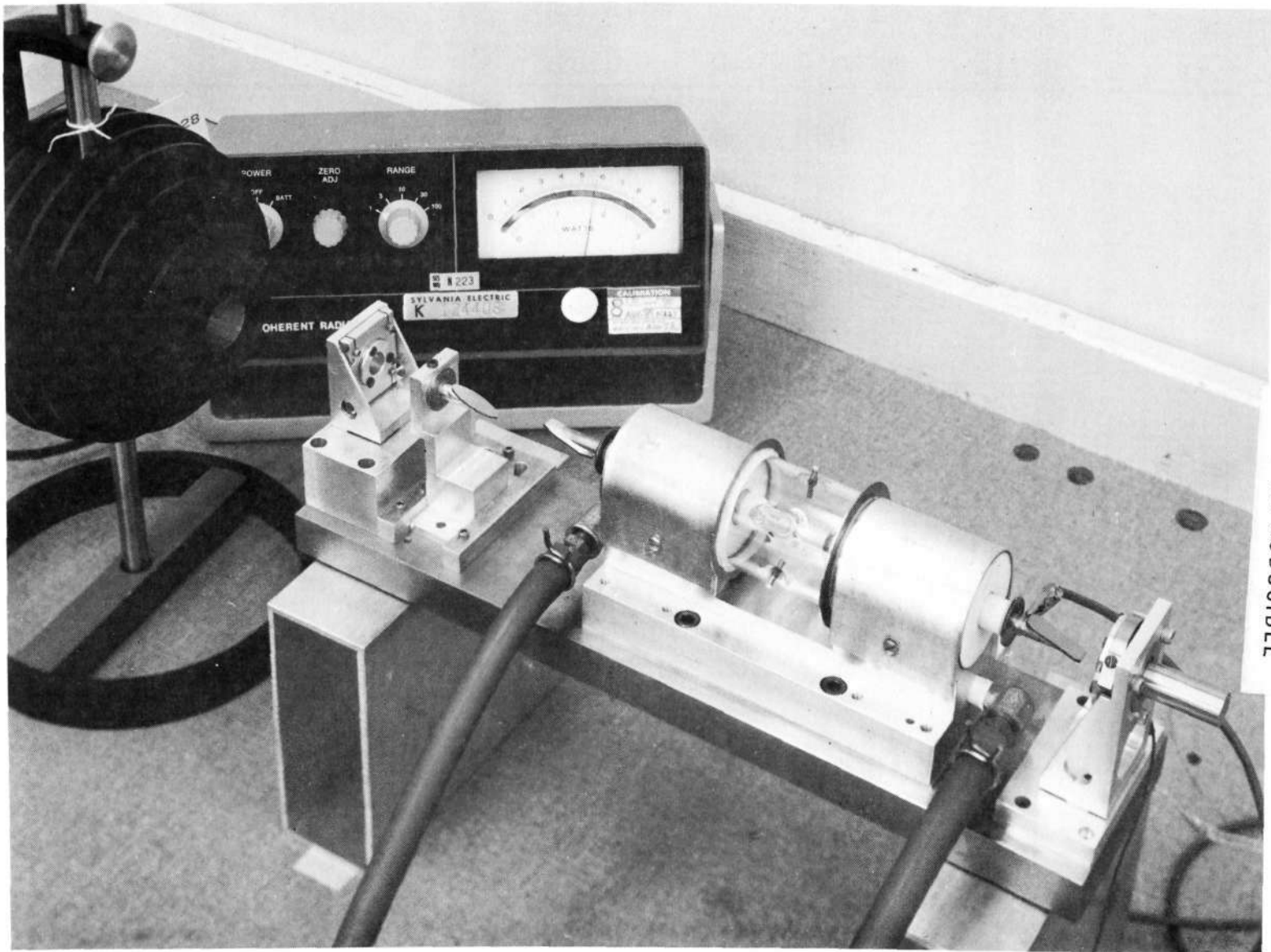


Figure 27 Pressure Increase Resulting From Heating $NiCO_3$.



NOT REPRODUCIBLE

Figure 28 Glass center section tube used for window testing

Upon failing it was removed from the Brewster window test fixture and subjected to the ATS-F sinusoidal vibration qualification levels. After vibrating it was leak checked and found to be leak-tight using a detector with a sensitivity of 6×10^{-10} STD-CC/sec of helium. Visual observation disclosed that a substantial amount of the black deposits formed in the cathode area during operation had been shaken loose.

This test demonstrated that a tube constructed with a glass center-section, using epoxy seals, has the potential for being space-qualified. The test also showed that the epoxy had not aged during the 5000 hours to the point where it became hardened or porous.

The vibration test also demonstrated that the NiO and carbon material formed on the cathode in tubes which have run for a long time can be shaken loose. In a zero G environment this material would be free to migrate to the Brewster windows and possibly reduce the laser output. Vibration of relatively young tubes, however, would most likely not demonstrate this problem.

SECTION 3

ALL-GLASS CO₂ LASER TUBES

3.1 INTRODUCTION

As mentioned in Section 2.2.4, the presence of glass in CO₂ laser tubes has been considered beneficial to tube life because of its ability to hold water vapor. Prior to the start of this program NASA Goddard personnel developed an all glass tube design capable of being space qualified. Sylvania was tasked to fabricate nine of the NASA tubes on the current program using an appropriate cathode design for the tube geometry chosen. Although no formal fabrication and process specifications were to be developed for these tubes, the process specifications used for the metal-ceramic tubes were to be applied wherever applicable. Sylvania also was to design and fabricate nine life test cavities (test benches) for delivery with the tubes. All testing efforts for these tubes have been conducted by NASA and will therefore not be discussed in this report.

The following sections discuss the general design of the tubes and associated hardware and present the planned variations in gas mixtures which were adopted for the tubes.

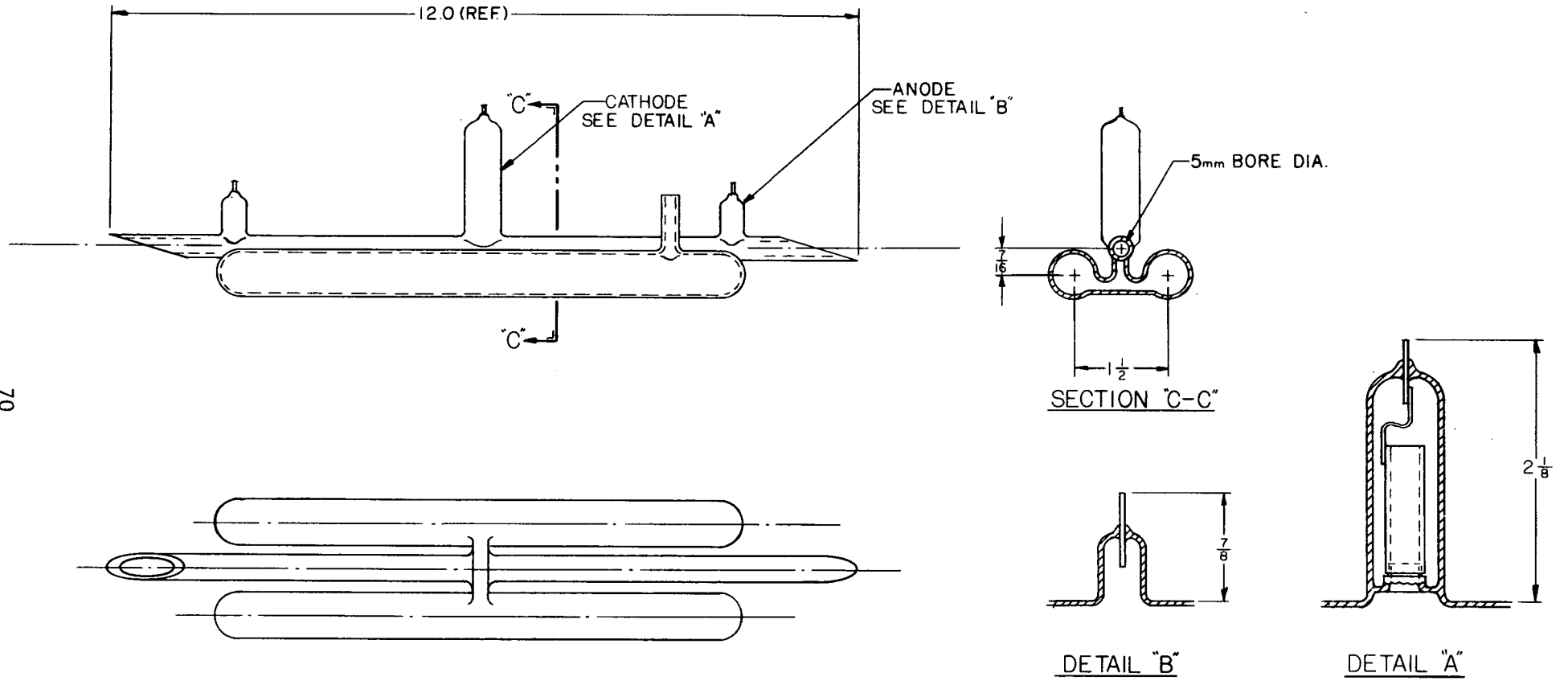
3.2 GLASS TUBE DESIGN

The tube design consists of a pyrex glass tube potted into the aluminum heat sink using a space qualified potting compound. Cooling of the bore is accomplished by conducting the heat through the potting compound to the aluminum heat sink. Figure 29 is a sketch of the glass tube. It has a nominal 5 mm diameter pyrex bore, two parallel Brewster angle windows of GaAs, two gas ballast pontoons, and two anode pins and a single cathode. The total tube gas storage volume is approximately 75 cc. A photograph of the tube is shown in Figure 30. The cathode is a nickel cylinder, platinum plated on the outside with an emission surface area of 5.5 cm². Samples of the final design for the cathode-glass assembly were sent to NASA and successfully vibration tested before incorporation in nine life test tubes.

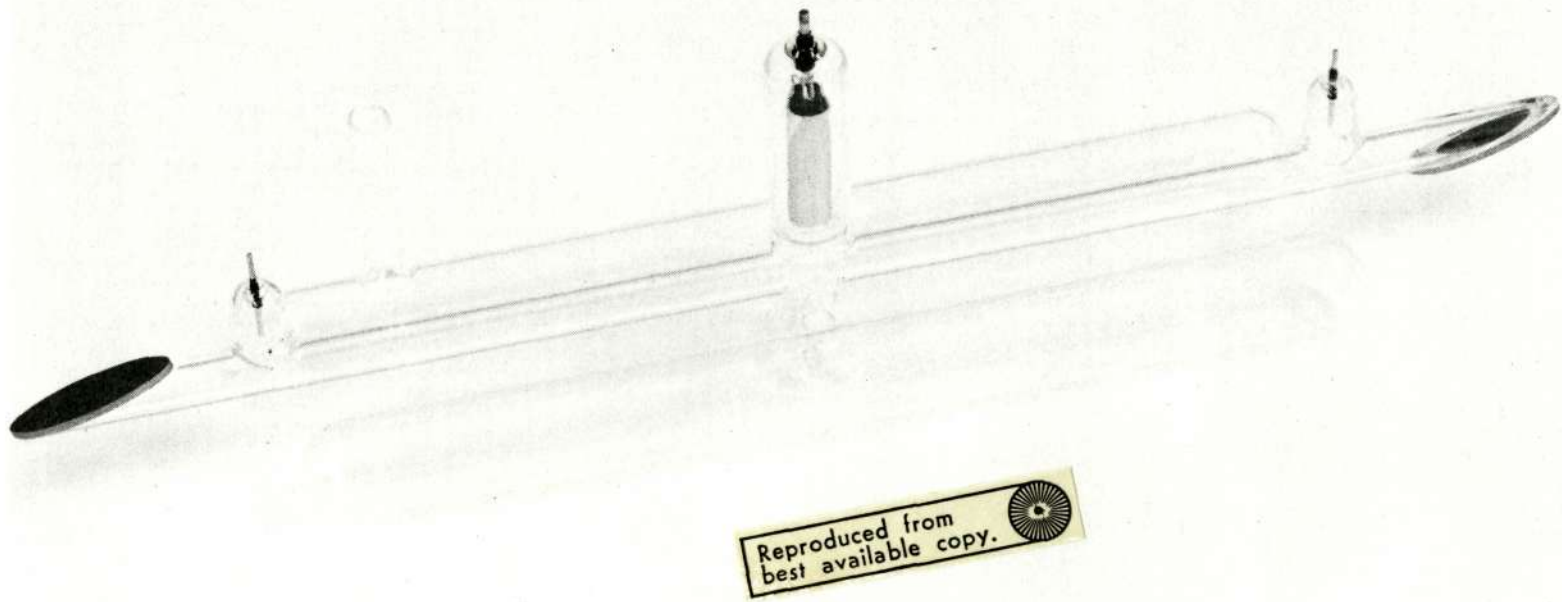
Figure 31 shows an assembly drawing of the aluminum heat sink. It consists of a base cavity, a cover, three aluminum risers, and three caps. The tube is assembled in the heat sink with teflon washers holding it on axis at both ends. Then the potting compound is added and allowed to cure.

PRECEDING PAGE BLANK NOT FILMED

Figure 29 Glass Life Test Tube



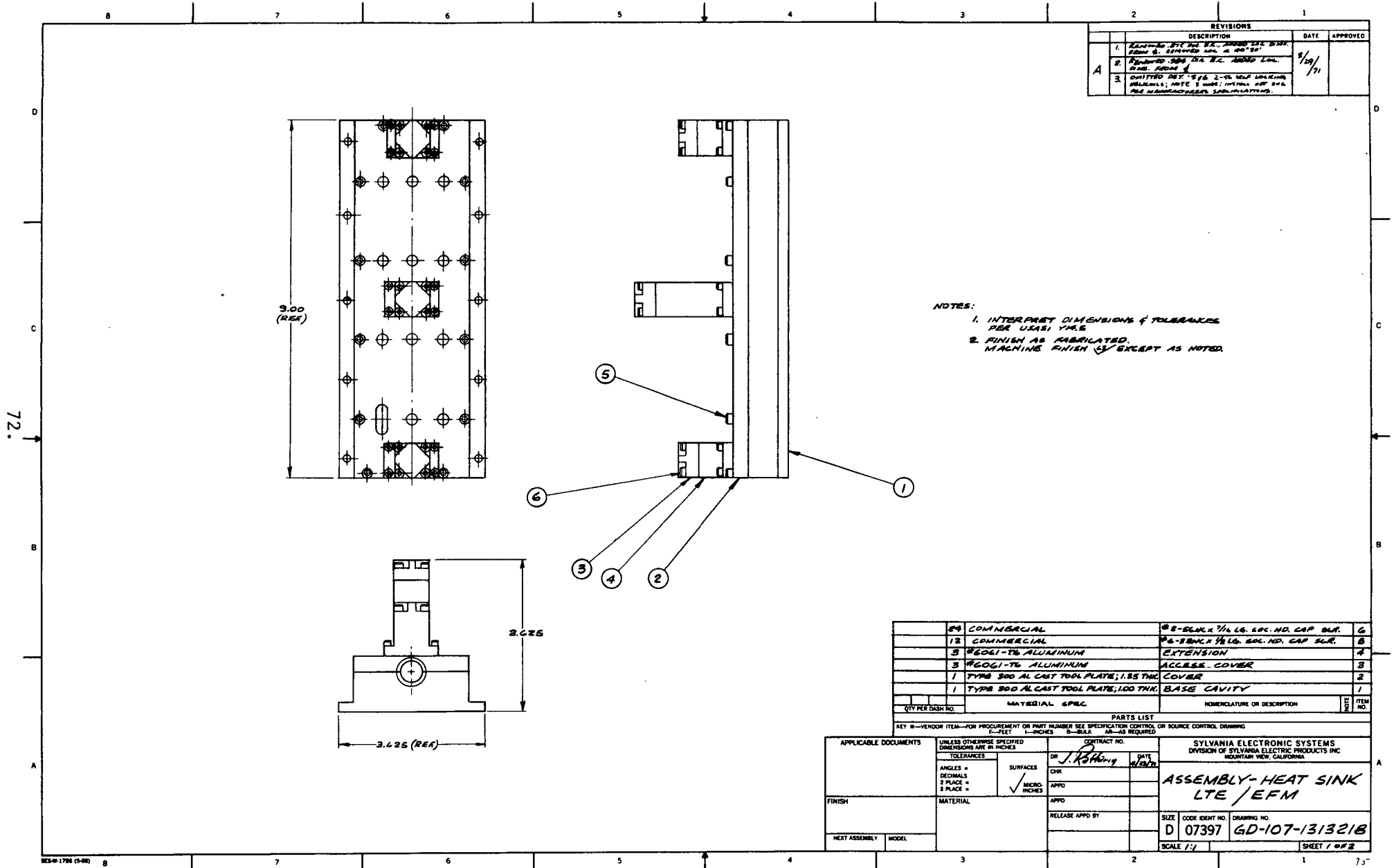
70



Reproduced from
best available copy. 

Figure 30 Photograph of all-glass tube

Figure 31 Assembly drawing of aluminum heat sink



REVISIONS			
	DESCRIPTION	DATE	APPROVED
1	REVISION #17 FOR M.T. APPROVED FOR DRAWING & REVISIONS FOR 4 1971		
2	REVISION #20 FOR M.T. APPROVED FOR DRAWING & REVISIONS FOR 4 1971	4/19/71	
3	CHANGED PART #16 2-12 NEW DRAWING (MATERIAL); NOTE 3 MODIFIED; MATERIAL APP #16 FOR MANUFACTURING SUBSTITUTIONS.		

- NOTES:
1. INTERPRET DIMENSIONS & TOLERANCES PER UNAS1 YMC
 2. FINISH AS FABRICATED. MACHINE FINISH \checkmark EXCEPT AS NOTED.

QTY PER DASH NO.	MATERIAL SPEC.	NOMENCLATURE OR DESCRIPTION	ITEM NO.
		#2-BLANK 7/16 LG. SOC. NO. CAP. CLR.	6
		#6-BLANK 7/16 LG. SOC. NO. CAP. CLR.	5
		EXTENSION	4
		#6061-T6 ALUMINUM ACCESS COVER	3
		COVER	2
		TYPE 300 AL CAST TOOL PLATE; 1.55 THK. BASE CAVITY	1

APPLICABLE DOCUMENTS	UNLESS OTHERWISE SPECIFIED DIMENSIONS ARE IN INCHES TOLERANCES	CONTRACT NO.	SYLVANIA ELECTRONIC SYSTEMS DIVISION OF SYLVANIA ELECTRIC PRODUCTS INC MOUNTAIN VIEW, CALIFORNIA
FINISH	ANGLES = DECIMALS = 2 PLACE = 3 PLACE =	DR <i>J. Robbins</i> DATE <i>4/19/71</i>	ASSEMBLY- HEAT SINK LTE / EFM
NEXT ASSEMBLY	SURFACES <input checked="" type="checkbox"/> MICRO INCHES	CHK APPD	
MODEL	MATERIAL	RELEASE APPD BY	SIZE CODE IDENT NO. DRAWING NO. D 07397 GD-107-131321B
			SCALE 1/1 SHEET 1 OF 2

3.3 GLASS LIFE TEST LASERS

Figure 32 is a photograph of a glass life test laser mounted on its life test bench during processing. The life test benches designed for use on the program were quite simple consisting of an aluminum base, two commercially available mirror mounts, and a water-cooled mounting block. The optical cavity consists of a metal-dielectric coated high-reflectivity non-output mirror with an 84 cm radius of curvature. The non-output mirror is mounted on a monolithic disc bender capable of providing cavity length changes of up to 15 microns. The output mirror consists of a 5% transmitting dielectric coating on a plane-parallel GaAs substrate. This mirror configuration was chosen to provide a required output beam divergence of 0.2° with a mirror separation of 14 inches. With these cavities the nominal power output was 2.0 watts multimode using a gas mixture of 0.1 Torr H_2 , 1.0 Torr Xe, 5.0 Torr N_2 , 5.0 Torr CO_2 , and 10.0 Torr He. Operating voltage at 10 ma total cathode current was about 2300 volts.

The potting compound used was Solithane formulation number Six available from Thiokol Chemical Corporation. The hardness of the material can be controlled by varying the resin to catalyst ratio. Some difficulty with glass cracking during the bake-out cycle on the early tubes was seen with the harder compositions, especially when the potting material was loaded with aluminum powder to increase its thermal conductivity. Thermal tests later indicated that the aluminum powder did not significantly change the thermal characteristics of the solithane and in fact was not required for acceptable laser power output. The bore temperature at the operating tube current ran at about $50^\circ C$ both with and without the aluminum filler.

Two variables were chosen for these tubes. One involved changing the amount of CO_2 and the other involved running a cathode in a separate discharge chamber for about 100 hours prior to installing it into the laser tube. During the preprocessing discharge, the cathode was heated to $330^\circ C$ using an RF induction coil.

Table 4 lists the nine tubes fabricated on this program, their designation, and their processing variations.

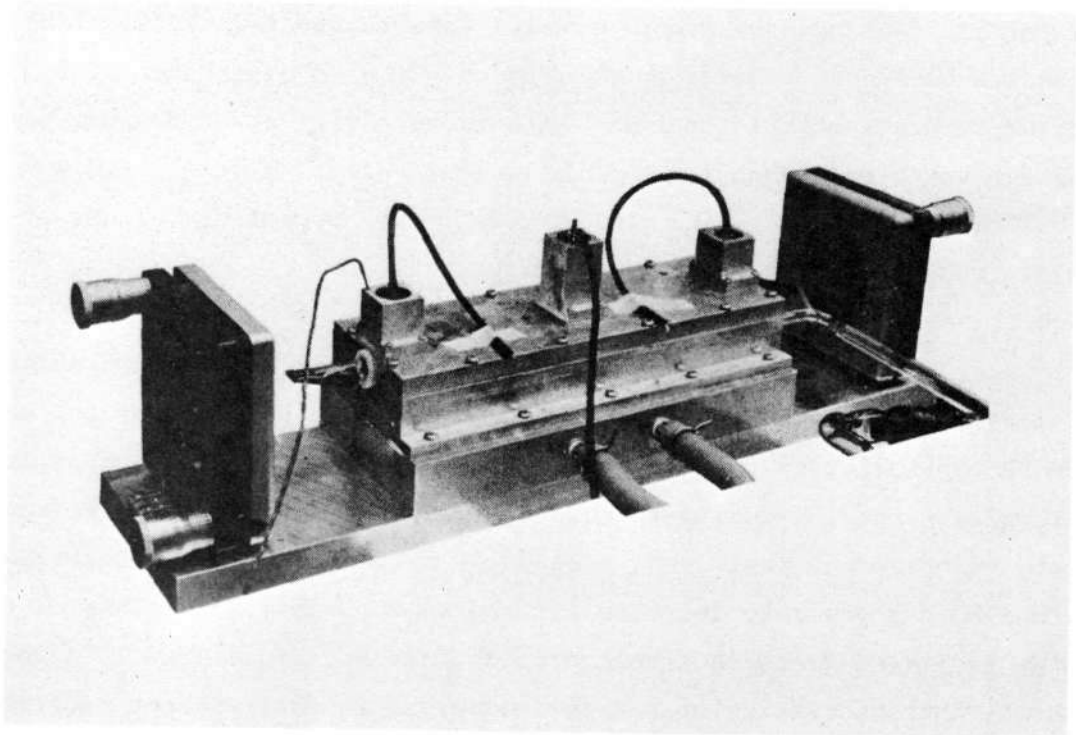


Figure 32 Completed glass life test laser with optical cavity

#	Designation	Process Variation
1	GT-1	Standard Mixture
2	GT-2	Standard Mixture
3	GT-3	Standard Mixture
4	GT-4	50% Additional CO ₂
5	GT-5	100% Additional CO ₂
6	GT-6	100% Additional CO ₂
7	GT-7	50% Additional CO ₂
8	GT-8	Preprocessed Cathode - 50% Additional CO ₂
9	GT-9	Preprocessed Cathode - Standard Mixture

Standard Tube Mixture: 0.1 torr H₂
 1.0 torr Xe
 5.0 torr N₂
 5.0 torr CO₂
 10.0 torr He

List of Glass Life Test Tubes and Their Life Test Variables.

Table 4.

SECTION 4

LASER CONTROL ELECTRONICS

4.1 INTRODUCTION

As part of the earlier LCE program an automatic frequency control unit for the laser subsystem was designed and fabrication was partially completed before the LCE program was terminated. Since the unit was near completion, a small additional effort was applied under this program to complete the electronics to an operational level. Although high-reliability parts were not used in this unit, all parts chosen have hi-rel counterparts.

4.2 SUMMARY OF ELECTRONICS SPECIFICATIONS

The frequency stabilization electronics are designed to accept the output of a bolometer, which is viewing a sample of the laser output power through some wavelength selection optics, and to control the laser frequency by means of the piezoelectric element supporting a cavity mirror until the laser is operating on the center of the doppler profile of the desired wavelength. To accomplish this, a system such as shown in the block diagram of Figure 33 is used. Also shown in the figure is the partitioning of the functions onto the five cards.

The electronics are designed so that when dc power is applied, the laser mirror transducer will oscillate in an axial direction with an amplitude of at least $\lambda/2$ at a rate of about 1/2 Hz. During a portion of this scan, the proper wavelength will be emitted by the laser and detected by the bolometer. When the power from the laser reaches a preset threshold level, the slow scan will be inhibited and the electronics will lock the laser frequency to the laser line center with the "dither" frequency control loop. If thermal expansion of the laser cavity becomes too large for the transducer range, the control loop will automatically drop out of lock and search for a better transducer position on a different laser axial mode.

Some of the salient interface specifications of the unit are shown in Table 5.

PRECEDING PAGE BLANK NOT FILMED

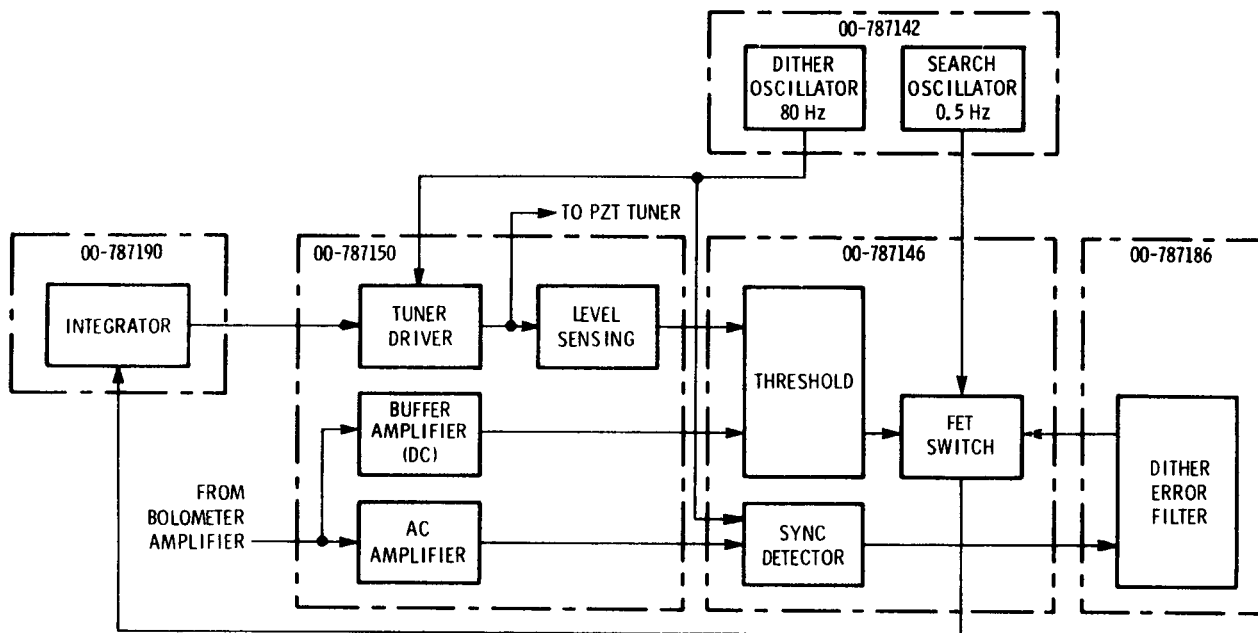


Figure 33 Frequency Stabilization Electronics

TABLE 5

MAJOR INTERFACE SPECIFICATIONS

Power Supply Voltage:		+ 250V
		+ 12V
		- 12V
		+ 5V
		- 5V
Power Consumption	less than	<u>1 watt</u>
Dither Frequency		75-80 Hz
Search Frequency		0.5 Hz \pm 20%
Peak Input Level from Bolometer		
Amplifier	Nominally	2.5V dc
Noise Density from Bolometer		
Amplifier	Nominally	1 μ V/ \sqrt Hz
Tuner Sensitivity:	"	8 MHz/Volt
Doppler Profile Width	"	100 MHz
Size:		6-1/4" x 4-1/2" x 3-3/8"
Weight:		2 lbs.

These interface specifications serve only as a guide for typical operation of the stabilization loop. The electronic control can accommodate a wider range of laser parameters and bolometer parameters with some accommodations in closed loop bandwidth and peak dither deviation. The target loop bandwidth is about 8 Hz and the peak dither deviation about 300 KHz.

4.3 STABILIZATION ELECTRONICS TEST RESULTS

The final packaging of the control electronics is shown in Figures 34 and 35. The dimensions, excluding connectors, are 6.14" x 4-1/2" x 3-1/4" high. The 3-1/4" dimension includes the 1/2" flange which has been provided for mounting on a suitable pedestal. The packaging dimensions and connector locations have been chosen to be compatible with the proposed layout for the NASA designed Laser Technology Experiment.

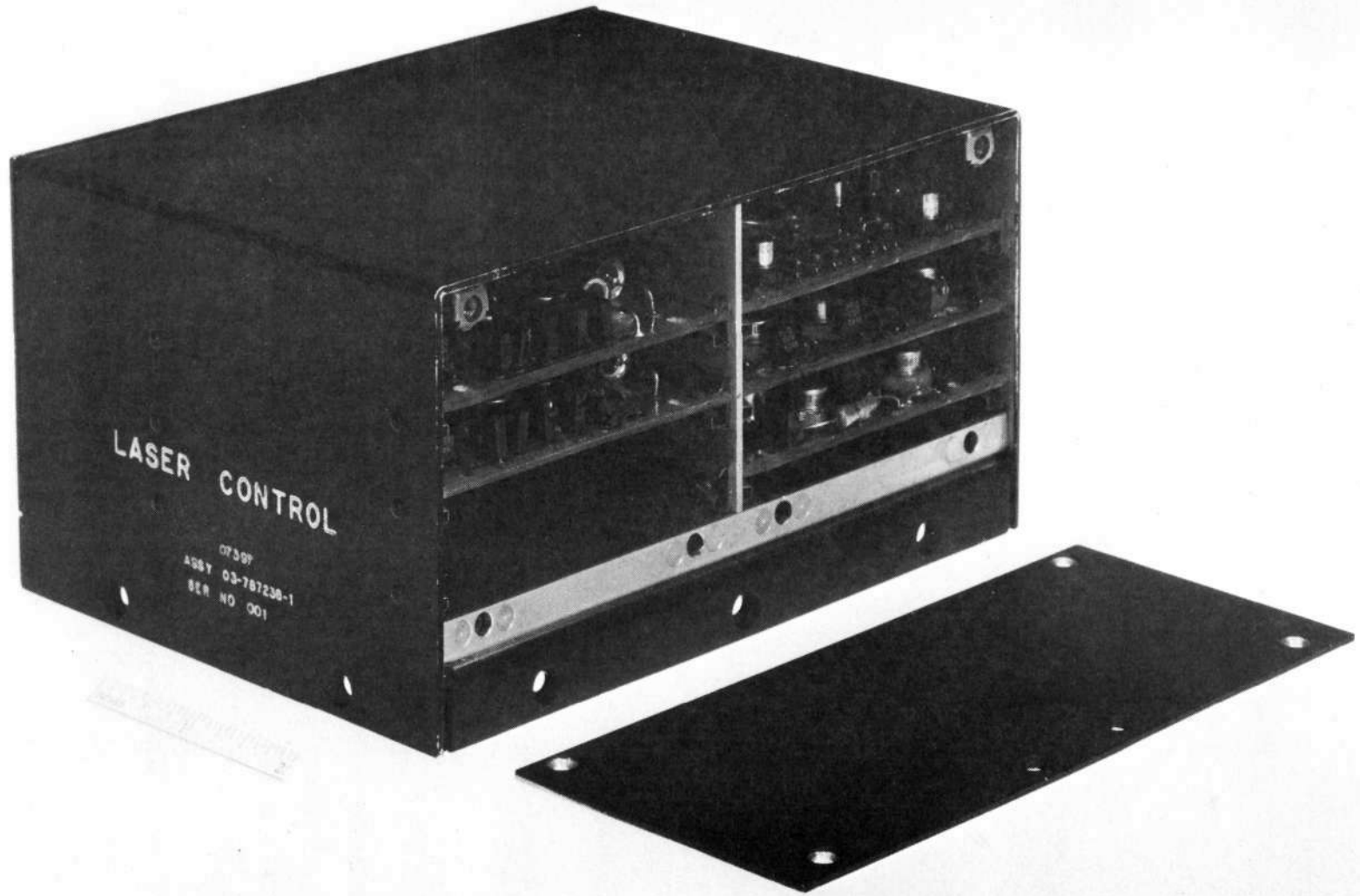


Figure 34 Photograph of the laser control electronics, front view

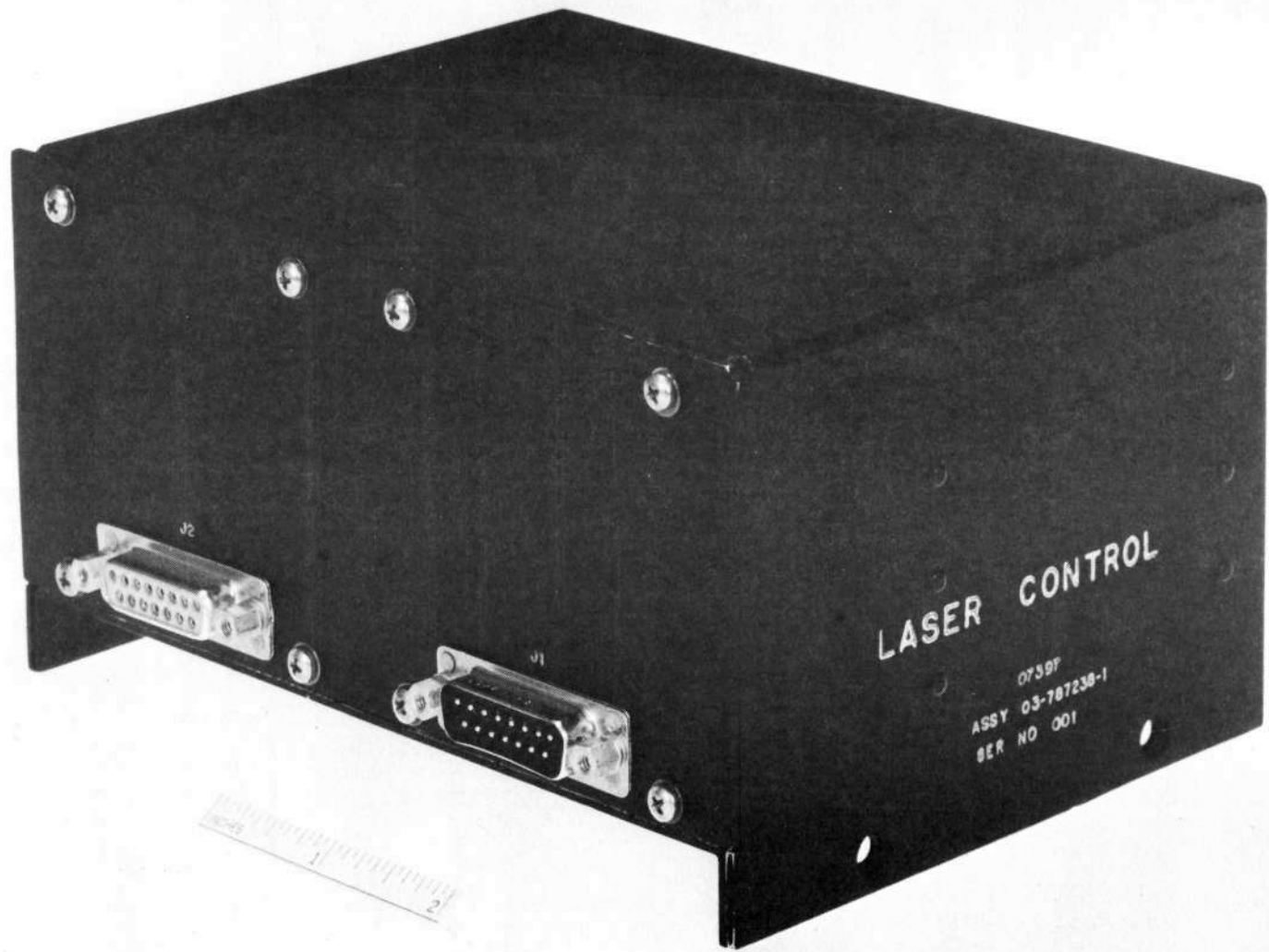


Figure 35 Photograph of the laser control electronics, rear view

The weight of the unit with cards and lid in place was measured to be 760 gm (1.68 lbs.).

Power supply currents with the unit operating normally are as shown in Table 6.

TABLE 6
POWER SUPPLY CURRENTS

<u>Voltage</u>	<u>Current</u>	<u>Max. Power</u>
+ 250V	2 mA	500 mW
+ 12V	10 mA	120 mW
- 12V	2 mA	24 mW
+ 5V	24 mA locked, 42 mA unlocked	210 mW (max.)
- 5V	14 mA	70 mW
		<hr/> 924 mW

The maximum power drain is seen to be less than 1 watt.

The operation of the unit was checked out with the aid of a "laser simulator". This unit, using FET's with a common drain resistor and with push-pull gate drives derived from the tuner voltage, simulates the output voltage from the bolometer amplifier which would result from scanning the laser frequency across the laser gain curve by varying the tuner voltage.

The stabilization electronics were demonstrated to be able to search and lock on the simulated Doppler profile. The dither amplitude and the threshold level adjustments ranges were measured with the results as follows:

dither amplitude (at tuner driver output)	50 mV p-p to 900 mV p-p
threshold level	< 0 V to greater than + 2.0V

The range of the inhibit circuit was observed to be 48V to 145V on the output of the tuner driver. The dither frequency was 77 Hz and the sweep period was 2.25 sec.

The loop was demonstrated to be able to lock stably with the laser simulator with the minimum dither amplitude. This value, 50 mV p-p, would represent typically a frequency deviation of 400 KHz p-p or 200 KHz peak if the laser tuning sensitivity is the nominal 8 MHz/volt. This value is below the nominal target value of 300 KHz peak deviation.

SECTION 5

CONCLUSIONS AND RECOMMENDATIONS

During the course of this program nine new metal-ceramic CO₂ laser tubes and nine all glass CO₂ laser tubes were constructed for the purpose of determining their life characteristics. Since the life testing of the glass tubes was not performed by Sylvania on this effort, no conclusions will be drawn at this time for the glass tubes, except that with the design features worked out during this program it now appears feasible to proceed with the formal development and space qualification of an all-glass laser tube if so desired. As far as fabrication and operating characteristics are concerned, the glass tube appears to have no major difficulties. The following paragraphs relate the major results, conclusions and recommendations applicable for the metal-ceramic tube.

The standard design metal-ceramic tube which uses a nickel cathode and 150 cc of gas storage volume is capable of operating for 400-600 hours before failure. Addition of pyrex glass (90 cm²) within the standard tube (a possible source of water vapor) does not significantly affect tube life. However, addition of extra CO₂ to the initial fill can increase tube life. With a 50% overfill of CO₂ we obtained more than 50% increase in tube life to about 825 hours. This was achieved, however, with a sacrifice of about 20% in initial power. Using a standard gas mixture but increasing the tube gas storage volume to 500cc, lifetimes in excess of 2000 hours were demonstrated in the present design without sacrificing laser power or efficiency. However, additional weight and volume are required. The two tubes under test which utilized the additional gas storage reservoir had dropped to about 75% of their initial power at the end of the 2000 hour test period. It should be noted that the volume increase of about 230% resulted in greater than 340% increase in tube life.

The data obtained with these test lasers along with other lasers tested earlier, strongly suggests that the most rapid fundamental life limiting effects which clean up the CO₂ gas in these tubes can be saturated so that the rate of CO₂ disappearance can be significantly reduced. From the

PRECEDING PAGE BLANK NOT FILMED

failure analysis data taken on this program (see Section 2.4 for details) we conclude that the oxygen provided to the tube volume by the breakdown of CO_2 chemically combines with the nickel cathode to form nickel oxide. It also appears that carbon and/or nickel-carbon compounds collect at the cathode surface. As the NiO and carbon compounds are formed they tend to protect the surface from further oxidation, slowly reducing the rate at which oxygen is chemisorbed. However, with the formation of these materials, which primarily form in porous nodules with very large surface area, large amounts of the other tube gases, especially CO_2 , CO, and O_2 are adsorbed onto the cathode surface. The temperatures at which the cathode operates (approximately 300°C) is not high enough to prevent this surface adsorption from occurring.

Therefore, early in tube life, oxygen is removed at a fairly high rate through the formation of NiO. Then as the NiO builds up, the other gases are selectively removed by adsorption. As the cathode surface becomes covered with NiO and carbon, the adsorption process appears to approach saturation if enough CO_2 molecules are present in relation to the cathode size. The process will never completely saturate, however, since cathode sputtering will always act to slowly remove the NiO-carbon surface and deposit it in other locations in the tube.

Measurements of Brewster window transmission, after the tube has operated for 2000 hours, does show a small but significant buildup of contaminant material on the inside surface of the windows most likely originating from the cathode. It appears as if the rate of buildup of this material alone would limit tube life to between 5000 and 10,000 hours.

An interesting phenomenon observed during the course of these life tests, which tends to confirm the failure mechanism proposed, was that all of the tubes which had dropped significantly in power could be rejuvenated to their original power. By boosting the cathode current by about a factor of 2 for about 30 minutes, thus raising the cathode temperature to about 400°C , most of the adsorbed gases could be liberated from the cathode to allow normal tube operation for an additional 50 to 300 hours. This rejuvenation process can be repeated as often as necessary allowing tube operation at near original power for 2000 hours or more.

Further conclusions which might be drawn from the above data, are that it may be advantageous to operate the nickel cathode at somewhat lower temperature than the 300°C now used. This would not only reduce the rate of NiO formation but also the rate of adsorption of the other gases. Preprocessing of the nickel cathode in a CO₂ environment prior to installation in the tube would also be advantageous.

It appears however, that to obtain tube life-times in excess of 5000 to 10,000 hours, a new cathode material will be required. This new material must exhibit a satisfactory combination of:

- a) low chemical reaction rate, at least after any preprocessing or passivation efforts,
- b) low sputtering rate of the basic material,
- c) low sputtering rate of the compounds which are formed on the cathode surface and
- d) low adsorption characteristics.

Although the nickel cathode provides quite a good combination of the above desired characteristics it must be improved upon if very long lifetimes are to be realized in small-sized CO₂ laser tubes. Given freedom of choice on tube size and therefore gas storage volume, the nickel cathode can provide excellent life characteristics. Lifetimes in excess of 10,000 hours have been demonstrated on earlier programs.⁽⁶⁾

Although shelf-life information is still limited for the metal-ceramic tube, the tests run here have shown that there is no significant reduction in tube capabilities for a shelf period under laboratory ambient conditions of at least 3000 hours (4-1/2 months). We feel this period of testing is long enough to determine that there are no significant chemical adsorption, or contamination problems occurring outside of the discharge area and the fundamental materials used in the current metal-ceramic tube design have no deleterious effects on tube life over long storage periods.

A possible alternate approach to achieving long-life without the use of a bulky gas storage reservoir involves the use of a solid state CO₂ generator. Preliminary studies on this program indicate that NiCO₃, when

heated to about 300°C irreversibly gives off large quantities of CO₂. Periodic heating of a chamber filled with NiCO₃ may be a very satisfactory way of maintaining the CO₂ partial pressure. Further research must be done with NiCO₃ or other source of CO₂ to determine its effects on other tube gases, and to determine the best techniques for maintaining the appropriate CO₂ level.

Our studies on techniques for maintaining a constant partial pressure of water vapor in the tube using Zeolite showed that the small pore size variety of Zeolite is indeed an effective sponge for water vapor. The Linde type 3A variety very effectively absorbs large quantities of water vapor preferentially over other tube gases. By controlling the Zeolite temperature to within a few degrees, the water vapor content in the tube can be accurately controlled and maintained. Short-term life tests in a CO₂ laser with Linde 3A Zeolite, however, indicated that although the water vapor could be controlled, other tube gases were slowly being absorbed by the Zeolite so that over a several day period a substantial drop in total tube pressure was noted. These tests indicated that a fairly complex preprocessing cycle would have to be developed before Zeolite could be used effectively.

SECTION 6

NEW TECHNOLOGY

During the performance of this program no items of new technology were developed.

SECTION 7

REFERENCES

1. W. J. Witteman and H. W. Werner, *Phys. Letters* 26A, 454 (1968).
2. Handbook of Electron Tube and Vacuum Techniques, F. Rosebury, Addison-Wesley Pub. Co., Inc. Reading, Mass., pp 13-14, 1965.
3. Engineering Materials Handbook, C. L. Mantel, McGraw-Hill Book Co. 1958, pp 36-41.
4. Advances in Catalysis and Related Subjects, Academic Press, Vol. 20, pp 167-266, 1969.
5. Catalysis by Metals, G. C. Bond, Academic Press, pp 553-557, 1962.
6. For example on contract NAS5-21537, GTE Sylvania recorded 15,000 hours of operation on an all-glass CO₂ laser tube with 600 cc volume and a heated nickel cathode. (Final Report, "Space Qualified CO₂ Laser," August 1971).

PRECEDING PAGE BLANK NOT FILMED

APPENDIX

Report No. 171160 prepared by Sloan Research Industries Inc. presents the techniques used, and the data, and results obtained from the x-ray diffraction studies performed as part of the failure analysis of the final precursor tube, R&D-1.

Report No. 177090 present the results obtained from x-ray diffraction, and emission spectrographic studies performed on the deposits formed on the cathode and quartz supports of MC-STD-5.

**SLOAN
RESEARCH
INDUSTRIES INC.**

2030 Alameda Padre Serra
Santa Barbara, Calif. 93103
805/965-0812



Report No. 177090

THE ANALYTICAL STUDIES OF CONTAMINATION
OCCURRING ON A CATHODE AND CATHODE SUPPORT

Introduction

On August 23, 1971 a nickel cathode and a quartz cathode support were received in the laboratory for analytical studies. It was requested that the dark contamination deposits appearing on the inside surfaces of the pieces be analyzed by X-ray diffraction and emission spectrographic techniques. Of special interest were determination of carbonates and copper compounds. The following report represents the results of the studies and is hereby respectfully submitted.

Sample Preparation and Study Methods

The sample preparation to obtain the samples for both of the analytical studies consisted of the following techniques: The inside surfaces of both pieces were covered with a 5% cellulose nitrate/amyacetate solution. When the cellulose nitrate was dry it was loosened by steam permeation. On the quartz support it was possible to merely pull the cellulose nitrate film off with large pieces of the deposit adhering to it; however, on the nickel cathode the cellulose nitrate film could not be pulled off. For this sample it was therefore necessary to resoften the film with amy acetate and then scrape it off with a probe while wet. Portions of the deposit were scraped off at the same time. With the cellulose nitrate effectively acting as a binder it was possible to roll the mixtures into .1mm diameter fibers which were then studied in a Debye-Scherrer Powder Diffraction Camera according to the following exposure conditions:

Kilovolts Potential	30
Milliamps	15
Target	Chromium
Filter	Vanadium
Pinholes	.025/.025-TS/SS
Film Type	Ilford Industrial G Type No Screen X-ray Film

Exposure	6 hours
Development	4 minutes/68°F in Eastman D-19 Developer

After the diffraction camera studies the same fibers were then sent to Pacific Spectrochemical Laboratories for emission spectrographic studies using standard carbon arc electrode cup methods.

Discussion of the X-ray Diffraction Data

The enclosed X-ray diffraction film prints are contact prints of the original negatives. Phase identification was made by measuring the observed diffraction line spacing ($1 \text{ mm} = 2^\circ\theta$) and calculating the interplanar atomic spacing or d values. These were compared with standard data in the ASTM X-ray diffraction file.

The X-ray diffraction studies showed both samples to be composed of a major phase of elemental nickel and strong intermediate phases of the NiO form of nickel oxide. The nickel cathode showed the highest concentration of nickel oxide even though considerable nickel was unavoidably scraped from the cathode itself. There was no measurable amount (less than 1%) of any copper compounds. Special checks were made to be sure there were no overlapping lines for the patterns of NiCO_3 , $\text{Ni}(\text{HCO}_3)_2$ and $\text{NiCO}_3 \cdot 6\text{H}_2\text{O}$. There is interference with the highest intensity lines of NiC and Ni_3C ; however, none of the other lines show up for these phases. There is also no trace of the higher temperature oxide, Ni_2O_3 form. Except for a very faint line representing the highest intensity platinum reflection on the quartz support sample no other phases are found to measurable extent (less than 2%). The high silicon content of that sample is most likely due to the quartz itself and, as such, would be amorphous and could produce no diffraction pattern.

The emission spectrographic data is as follows:

Deposit from
Nickel Cathode

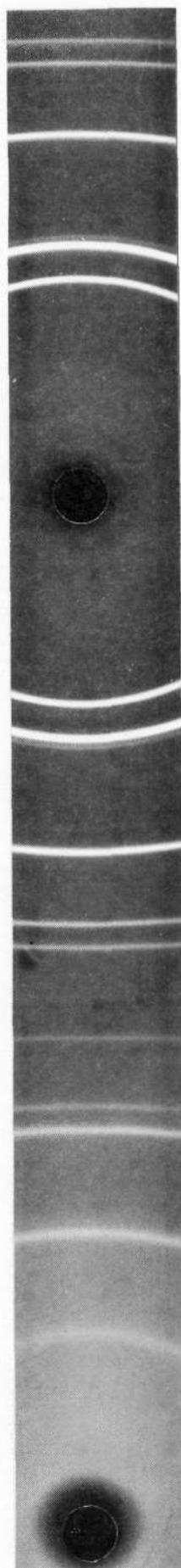
Ni-	78.8
Si-	0.24
Pt-	0.30
Mg-	0.0091
Fe-	0.033
Cu-	0.0025
Ca-	0.014
Cr-	0.0051
Other elements	nil

Deposit from
Cathode Support

Ni-	66.8
Si-	5.8
Fe-	0.43
Pt-	3.0
Mg-	0.019
Cu-	0.015
Co-	trace (less than 0.05)
Ca-	trace (less than 0.01)
Cr-	tract (less than 0.04)
Other elements	nil

Ni CATHODE MATERIAL

XRD Film Print 3871



**SLOAN
RESEARCH
INDUSTRIES INC.**

2030 Alameda Padre Serra
Santa Barbara, Calif. 93103
805/965-0812

sloan

Report No. 171160

**THE X-RAY DIFFRACTION STUDIES
OF CONTAMINATIONS OCCURRING
ON A CATHODE AND CATHODE SUPPORT**

Introduction

On June 4, 1971 a nickel cathode and a quartz cathode support were received in the laboratory for X-ray diffraction studies. Studies were made of the black contamination found on the inside diameter of both pieces and the green contamination found on the edge of the quartz cathode support. The following report represents the results of these studies and is hereby respectfully submitted.

Sample Preparation and Study Methods

The deposits on the inside diameters were flaky and it was possible to remove areas by merely lightly scraping with a probe. The material thus removed was mixed with a 5% solution of cellulose nitrate in amyl acetate. When the proper consistency was reached the mixtures were formed into .2 mm diameter fibers and used as samples in a Debye-Scherrer Powder Diffraction Camera. The green material was removed from the edge of the quartz cathode support by covering the surface of the deposit with a droplet of the cellulose nitrate solution and allowing it to dry. This composite was then peeled off with the aid of a razor blade with the cellulose nitrate acting as a binder. The mixture was resoftened with amyl acetate and formed into a fiber. The diffraction studies were made according to the following exposure conditions:

Kilovolts Potential	30
Milliamps	15
Target	Copper
Filter	Nickel
Pinholes	.025/.025-TS/SS
Film Type	Ilford Industrial G Type No Screen X-ray Film
Exposure	6 hours
Development	4 minutes/68°F in Eastman D-19 Developer

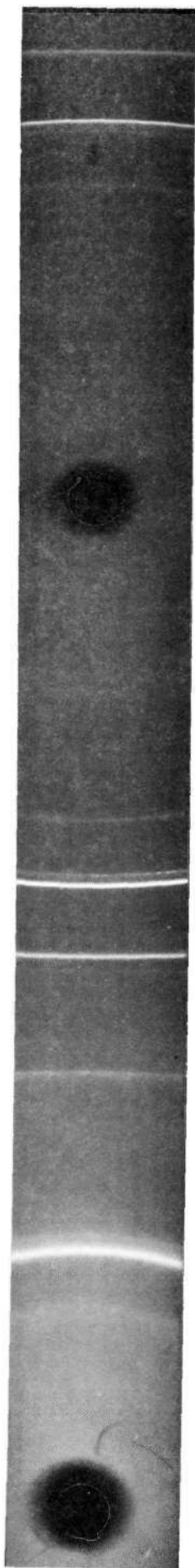
Discussion of the X-ray Diffraction Data

The enclosed X-ray diffraction film prints are contact prints of the original negatives. Phase identification was made by measuring the observed diffraction line spacing ($1 \text{ mm} = 2^\circ\theta$) and calculating the interplanar atomic spacing or d values. These were compared with standard data in the ASTM X-ray diffraction file.

All three areas show the NiO to be present in each area. Both of the inside diameter areas show in addition a pattern which most closely matches the CuSn inter-metallic. This pattern was previously interpreted and reported by telephone as elemental tungsten and tungsten sub-oxide; however, the copper/tin inter-metallic gives a better solution to the d-spacing values and intensities. The nickel cathode piece shows only a minor amount of CuSn while the quartz support shows approximately equal contaminations of the CuSn and NiO phases. The green deposit on the edge of the quartz piece contains a major amount of NiO form, a minor amount of the Cu_2O form of copper oxide and a trace amount of the CuSn inter-metallic.

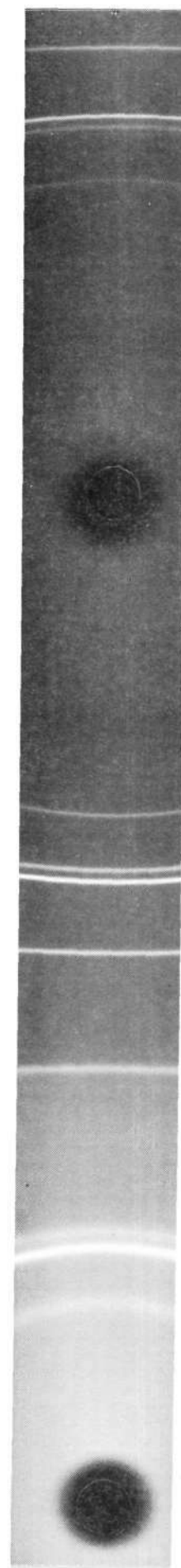
QUARTZ SUPPORT
DEPOSIT

XRD Film Print 3962



NICKEL CATHODE
DEPOSIT

XRD Film Print 3961



DEPOSIT FROM ID
OF QUARTZ CATHODE
SUPPORT

XRD Film Print 3872



GREEN MATERIAL
FROM QUARTZ
CATHODE SUPPORT

XRD Film Print 3873

